ACS ORGANIC & INORGANIC Au
AN OPEN ACCESS JOURNAL OF THE AMERICAN CHEMICAL SOCIETY

pubs.acs.org/orginorgau
Perspective

"Polytopal Rearrangement Model of Stereoisomerization" and Its Potential as the Basis for a Systematic Model of All Stereoisomerism

Peter J. Canfield,* Jeffrey R. Reimers,* and Maxwell J. Crossley*

Cite This: *ACS Org. Inorg. Au* 2024, 4, 356−372
Read Online
ACCESS | Metrics & More | Article Recommendations | Supporting Information

ABSTRACT: The term "polytopal rearrangement" describes any shape changing process operating on a coordination "polyhedron"—the solid figure defined by the positions of the ligand atoms directly attached to the central atom of a coordination entity. Developed in the latter third of the last century, the polytopal rearrangement model of stereoisomerization is a general mathematical approach for analyzing and accommodating the complexity of such processes for any coordination number. The motivation for the model was principally to deal with the complexity, such as Berry pseudorotation in pentavalent phosphorus species, arising from rearrangements in inorganic coordination complexes of higher coordination numbers. The model is also applicable to lower coordination centers, for example, thermal "inversion" at nitrogen in NH_3 and amines. We present the history of the model focusing on its essential features, and review some of the more subtle aspects addressed in recent literature. We then introduce a more detailed and rigorous modern approach for describing such processes using an assembly of existing concepts, with the addition of formally described terminology and representations. In our outlook, we contend that the rigorous and exhaustive application of the principles of the polytopal rearrangement model, when combined with torsional isomerism, will provide a basis for a mathematically complete, general, and systematic classification for all stereoisomerism and stereoisomerization. This is essential for comprehensively mapping chemical structure and reaction spaces.

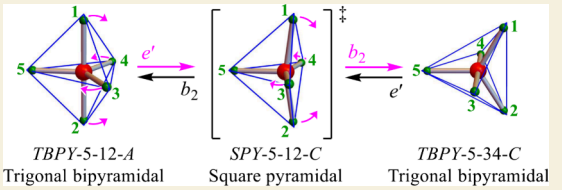

KEYWORDS: *Polytopal rearrangement, stereoisomerism, stereoisomerization, molecular geometry, chemical space, stereoisomerism classification, fundamentals of isomerism*

INTRODUCTION

Two centuries of chemical discoveries have led to the development of a sophisticated understanding of static and dynamic molecular structure. This includes a rich diversity of stereoisomerism phenomena and concepts that comprise an ad hoc collection. In seeking to see where our recently reported experimental demonstration of akamptisomerism[1] fitted within this broader context of stereoisomerism, we found that a single general and systematic classification does not exist. Attempting to devise such a classification system drew us to the "polytopal rearrangement model of stereoisomerization", which we review here.

A polytopal rearrangement is a real or conceptual shape-changing transformation that moves the vertices defined by the ligand atoms in a coordination polyhedron or polygon (the general term being a "polytope"). The development of the polytopal rearrangement model began in the 1960s by Muetterties[2−18] as a general approach[5] to describe and interrogate the possible mechanisms underlying the unexpected dynamical unimolecular stereoisomerization phenomena ("fluxionality") being discovered in numerous inorganic complexes.

One early success[5] of the model describes the "inversion" (more precisely called a geometric reflection) of tricoordinate trigonal pyramidal (*TPY*-3) species through a trigonal planar (*TP*-3) intermediate shown in general form in Figure 1a.

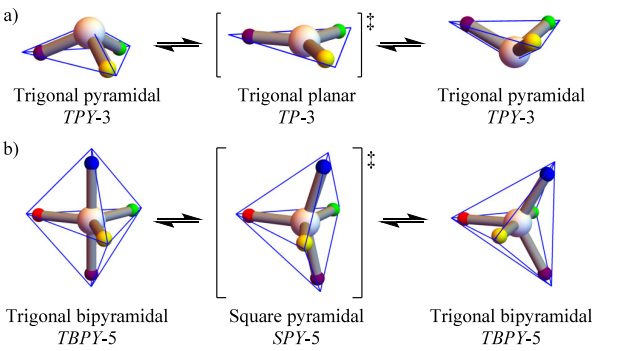

Figure 1. Two polytopal rearrangements in general form. Atom colors are for tracking purposes and do not denote specific chemical elements. The blue lines define the edges of the polytopes. (a) Geometric reflection (traditionally called "inversion") of a *TPY*-3 geometry via a *TP*-3 intermediate. (b) Berry pseudorotation process whereby *TBPY*-5 geometries interconvert through an *SPY*-5 intermediate.

Received: January 22, 2024
Revised: February 25, 2024
Accepted: February 27, 2024
Published: March 27, 2024

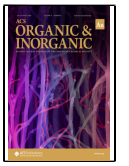

https://doi.org/10.1021/acsorginorgau.4c00005
ACS Org. Inorg. Au 2024, 4, 356−372

A second and important success[4] describes fluxionality in pentacoordinate trigonal bipyramidal (*TBPY*-5) species through a square pyramidal (*SPY*-5) species. This interconversion is shown in general form in Figure 1b.

Specific examples for tricoordinate species for the process shown in Figure 1a are the "inversion" of NH_3 and related amines.[19] For pentacoordinate species, specific examples include P(V) halides (Figure 1b)—this being called Berry pseudorotation.[20,21] While these examples involve coordination at a nonmetallic central atom, the geometry-changing processes are equally applicable to the far more numerous metallic elements. Additionally, metals generally have a potential for larger coordination numbers, hence development of the model gravitated toward a much wider application within the field of inorganic chemistry.[2−18,20−61]

Application of the model was historically motivated by the observation of thermally facile rearrangements at ambient temperature.[62,63] Given that rearrangement for carbon centers involves far higher energy barriers, the model was not generally applied to organic compounds and thus was not *universally* adopted for all chemical elements.

Facile polytopal rearrangements abound throughout chemistry and are of significant practical importance to transition metal-catalyzed reactions, where these types of rearrangements often occur in reaction-intermediate complexes leading to the products.[38,39,43,64,65] Such reactions are extensively used at both the laboratory and industrial scales.

Presented as a general approach for arbitrary *n*-coordination and geometries, the model was successfully applied to pentacoordinate phosphorus species[4,8,20−24] including chelating ligands.[25,26] The early work also examined the unusual case of pentacoordinate carbon species.[66] Further development of the model led to its generalization to describe dynamical behavior in tricoordinate p-block[27] species; tetracoordinate s-block,[28,29] p-block,[29−32] and d-block[29,33−37] species; pentacoordinate d-block[32,38−45] and further work on p-block[46−48] species; hexacoordinate d-block[7,49−54] and p-block[32,55] species; heptacoordinate general[18,32] and d-block[56−58] species; octacoordinate[14,32,57,59−61] species; and nonacoordinate[17] species. Interest in the model also stimulated the synthesis of numerous chemical systems designed to probe new or unresolved questions regarding polytopal rearrangement mechanisms.[25,26,42,47,67−70]

Historically, and with the emphasis on inorganic coordination complexes, the rearranging centers were written as "ML_n" where all L are "bonded" to M. Where appropriate to the historical context, we use ML_n. In a more general context, we adopt the form AB_n, where A and B are any atoms, and the B-atoms need not be the same.[32]

As the model describes dynamic and continuous geometry-rearrangement processes (stereoisomerization), *every* static geometry along a reaction path is implicitly described. In this Perspective, we propose that the polytopal rearrangement model has a powerful utility beyond it simply providing a means for analyzing real stereoisomerization phenomena, which has been its application to date. With a focus on the pure geometry aspects of molecular structure, we propose that the principles of the model — *when rigorously and exhaustively applied* - provides a systematic and comprehensive way to map out the full scope of geometric possibilities for any AB_n system.

We commence this Perspective by giving the history leading up to, and the development of, the polytopal rearrangement model of stereoisomerization, describing its essential features. Later, we review more recent work that addresses some of the subtleties of the model not appreciated in earlier works. These works also provide robust schemes for application of the model to modern interests. We then present the model using modern depictions and terminology designed to facilitate a precise and concise discussion, and to connect it with current concepts. This modern approach expands the principles of the model to accommodate all possible stereoisomeric geometries. Finally, in the Outlook section, the focus of our discussion turns to how the model steps us toward a complete description of stereoisomerism. As we enter this age where research is becoming increasingly dominated by computer-led approaches (including machine learning), this can only be of great benefit to the field of Chemistry,[71−73] including building a universal chemical reaction database.[74]

The Current IUPAC Definition

Formally, in the International Union of Pure and Applied Chemists (IUPAC) Compendium of Chemical Terminology (the "Gold Book"), the polytopal rearrangement model of stereoisomerization is defined as

> *"Stereoisomerization interconverting different or equivalent spatial arrangements of ligands about a central atom or of a cage of atoms, where the ligand or cage defines the vertices of a polyhedron. For example pyramidal inversion of amines, Berry pseudorotation of PF_5, rearrangement of polyhedral boranes."*

The inclusion of "*a cage of atoms... For example... polyhedral boranes*" in this definition is problematic as rearrangements of this type necessarily involve *changes* in bonding topology (atom connectivity) and hence, strictly speaking, are examples of *constitutional isomerization* and not stereoisomerization. As an example, the thermal rearrangement of 1,2-*closo*-dicarbadodecaborane to its 1,7-isomer (Figure 2) is an example of constitutional isomerization with both the isomers and any conceivable intermediates exhibiting differences in bond topology.

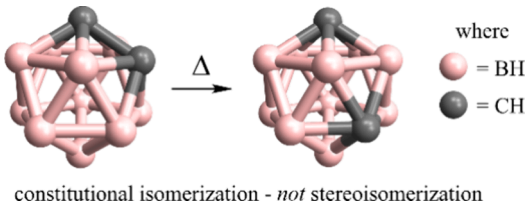

Figure 2. Rearrangement of the framework atoms of dicarbadodecaboranes necessarily involves changes in bonding topology and falls under constitutional isomerism and not stereoisomerism.

For the purposes of this Perspective on the polytopal rearrangement model of *stereoisomerization*, we concentrate exclusively on coordination centers "AB_n" and where all the A−B bonds are conserved and unchanging throughout and are thus strictly described as stereoisomerization. Nevertheless, the problem with this IUPAC definition indicates that the polytopal rearrangement model in fact has greater significance to isomerism more widely.

It is worth noting that in the context of polytopal rearrangements of AB_n the term "ligand" should be interpreted to simply mean an atom (B) bonded to a coordination center (A). Further, the type of bond between A and B is immaterial to the discussion.

https://doi.org/10.1021/acsorginorgau.4c00005
ACS Org. Inorg. Au 2024, 4, 356−372

MOTIVATION FOR THE MODEL

Research in chemistry surged in the 20th century, especially after World War II, with powerful investigational tools such as X-ray crystallography, electron diffraction, and NMR becoming widely accessible. While the stereochemistry of organic systems was largely known at that point, new studies on inorganic systems revealed a great diversity of structural possibilities and dynamical behaviors. Key to the discussion here was the elucidation of structures for numerous polyhedral boranes and metal "cluster compounds"; as well as fluxionality of $Fe(CO)_5$ and PF_5 along with other temperature-dependent "stereomutation" reactions of coordination complexes.[62,63,75,76]

It was in this environment that polytopal-rearrangements pioneer Earl Muetterties began his career in the 1950s. Some of his notable relevant early works included studies on numerous molecular fluorides; these focused on both their static structure and their fluoride-exchange dynamics as determined by ^{19}F NMR.[77−79] One study,[80] focused on ReF_7 and IF_7, described "intramolecular ligand exchange" processes, with another describing "intramolecular racemization" in pentacoordinate chiral compounds.[2] Additionally, Muetterties worked on polyhedral boranes[79,81,82] and it is reasonable to assume that the aesthetic appeal of their polyhedral structural forms had a direct influence on the later development of the model discussed here.

Notable developments by others that contributed conceptually were the 1955 invention of the ammonia maser,[83] which relies on *TPY*-3 "inversion", the 1958 report of fluxionality in $Fe(CO)_5$ by Cotton et al.,[63] Berry's 1960 description of "tunneling" to describe fluxionality in molecules such as NH_3 and PF_5,[84] Hoard and Silverton's 1962 analysis of the stereochemistry of octacoordinate centers[85] in which the transformation between square antiprismatic and dodecahedral geometries was described, and Lipscomb's 1966 work describing the framework rearrangement (constitutional isomerization) processes apparent in polyhedral carboranes.[86]

For simple compounds such as PF_5, the need to follow individual ligand atoms beyond their distinct positional character (e.g., axial or equatorial) was not pressing. Later, more complex derivatives were studied,[23,25,66,87] leading to compounds that were specifically designed to probe aspects of the dynamic "intramolecular stereoisomerization" of such systems.[20,47,70,88−94] Hence, the challenge to analysis grew markedly, and a more comprehensive treatment was demanded, not just to track the positions of individual atoms but also to follow and differentiate between the specific mechanistic transformation possibilities. To this end, the concept of "permutation stereoisomers" was employed.[4,5]

The mathematical fields of Combinatorics and Group Theory form the basis for generating *permutation stereoisomers*.[4,5] In simple terms, for an arbitrary coordination center AB_n exhibiting a characteristic geometry, the permutation stereoisomers are all the distinct ways that distinguishable B atoms can be arranged about A with the same general geometry; the permutation stereoisomers are the different possible "configurations".

The challenge then became one of conceiving mechanistic intermediates that transform a reference system to one or more of the permutation stereoisomers in a *single concerted* step. If the different potential mechanisms generate characteristic ligand-positional permutation *patterns*, then it follows that some mechanistic insights would be gained from the study of appropriate chemical systems. This was the starting point from which the polytopal rearrangement model was conceived.[4,5]

Vibrational Modes and Reaction Coordinate

A key physical picture that would later inform the polytopal rearrangement model is the idea that for *thermally activated* processes, like those shown in Figure 1, the stereoisomeric chemical entities occupy wells on the molecular potential energy surface that support vibrational zero-point motion.[95] This physics was central to Berry's 1960 paper[84] with molecular vibrational frequency, and the energy barrier to the reaction as parameters to the physics of the rearrangement. This concept was reiterated in diagrammatic form in Hoskins and Lord's 1966 report[96] of the vibrational spectra of PF_5 and AsF_5 (Figure 3).

Additionally, in Holmes and Deiters' 1968 discussion about pentacoordinate phosphorus halides, mention is made of the "low frequency and large amplitude [vibrational] motion (hence a correspondingly small force constant) associated with a molecule of comparatively low reduced mass".[87] This statement explicitly equates a vibrational molecular motion with the beginning of a reaction coordinate.

THE POLYTOPAL REARRANGEMENT MODEL

Initial Conceptual Framework

A first attempt at a comprehensive approach to understanding unimolecular stereoisomerization came in 1968 where Muetterties looked at ML_6 (AB_6) systems.[3] This early paper uses the term "polyhedral rearrangement" and introduced the concept of

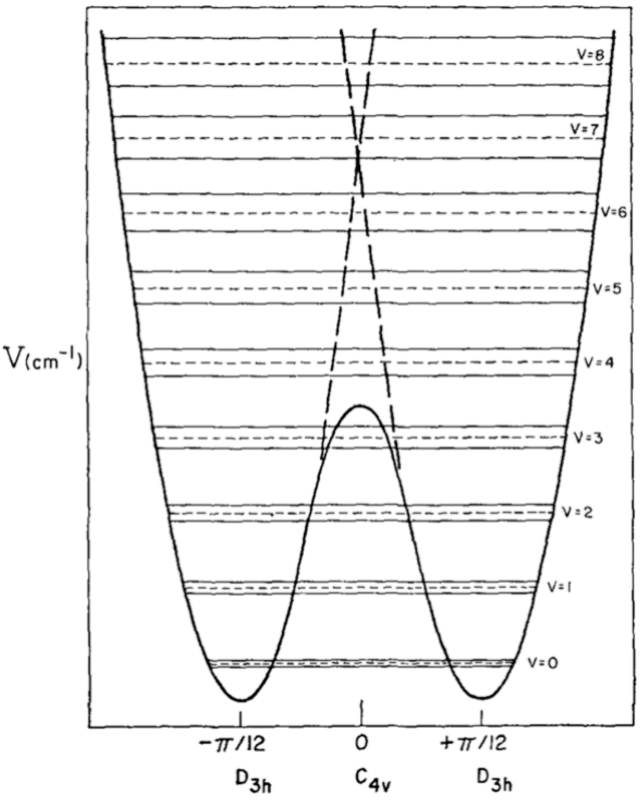

Figure 3. Hoskins and Lord's double-well potential energy diagram for a phosphorus pentahalide corresponding to a single Berry pseudorotation transformation. Vibrational levels are indicated (splitting of lower levels greatly exaggerated with the average energies indicated by the dashed lines). Reproduced with permission from ref 96. Copyright 1967 AIP Publishing.

https://doi.org/10.1021/acsorginorgau.4c00005
ACS Org. Inorg. Au 2024, 4, 356−372

the "topological representation" of stereoisomers. The topological representation of stereoisomers is a mathematical system for representing the relationships between all the different permutation stereoisomers for a given mechanism. Essentially, it embodies which permutation stereoisomers can interconvert directly through the stated mechanism by a single concerted step. Here, "topological" refers to the network of single concerted step relationships between the permutation stereoisomers—it does not refer to bond topology.

An analysis based upon this representation depends upon the distinguishability of the B atoms in AB_n. In a compound such as *TBPY*-5 PF_5, the axial and equatorial F atoms are distinguishable from each other, but the two axial atoms are indistinguishable from each other and, similarly, the three equatorial atoms are indistinguishable. Isotopic labeling, or using different chemical groups, introduces increased scope to distinguish the B atoms. In the most general case, all B atoms are assigned a distinctive index for the purposes of tracking, allowing a full analysis to be conducted.

Pairwise relationships indicating permutation stereoisomers that can be interconverted through a single concerted step emerge from this topological representation. These relationships are readily depicted as *graphs*: abstract objects central to the mathematical field of Graph Theory. The permutation stereoisomers are represented as nodes or *graph vertices*, and the pairwise relationships (stereoisomerization reactions) are represented as lines or *graph edges* between the vertices.

An example of a graph from Muetterties' 1968 paper[3] is shown in Figure 4a. This depicts the relationships between *tris* unsymmetrical-bidentate-chelate octahedral (*OC*-6) complexes of the form $M(a{-}b)_3$ that undergo stereoisomerization via trigonal prismatic (*TPR*-6) intermediate forms produced by either the Bailar twist mechanism[76] (Figure 4b) or the Ráy-Dutt twist mechanism[75] (Figure 4c).

The graph vertices in Figure 4a (labeled by Muetterties as "d-cis", "l-cis", "trans", etc.) positioned at the vertices of the tetrahedron (open circles) represent the four possible distinct *OC*-6 species, with the *TPR*-6 intermediates (black circles) between these. Note: the edges joining "d-cis" to "d-trans" and "l-cis" to "l-trans" have no feasible direct *TPR*-6 intermediates. Mathematically, these additional graph edges should not have been part of the graph and, indeed, the tetrahedral layout Muetterties used has debatable utility.

Seminal Publications on the Polytopal-Rearrangement Model

Muetterties followed up the 1968 paper[3] with the two seminal papers on the "Topological representation of stereoisomerism".[4,5] The first of these papers[5] laid out many of the foundational principles, with the second[4] focused on its implementation for the "five atom family" ("ML_5" and "M_5", though the latter actually involves constitutional isomerization).

Presented as a general approach to representing the relationships between permutation stereoisomers, these papers clarify several points from the 1968 paper to focus attention on the essential details. These are

- the atoms in ML_n (AB_n) are implicitly treated as point-like objects,
- the general shapes of the polytopes are idealized to high symmetry forms,
- the identity of the "atoms" is immaterial to the analysis,
- for the most general cases, the permuting atoms are each assigned a distinct index to track them, and
- any underlying physics in the model is only *implied* through consideration of a geometric transformation that changes one polytopal form into another.

A corollary of this latter point is that the model says nothing about the lifetime of any intermediate or the absolute rates of individual transformations.

With considerable insight, the first of these seminal papers[5] alluded to the significant scaling problem for an *n*-atom family as *n* increases and indicated that automated (computer) approaches would be needed.

This paper also briefly addressed the ML_3 (AB_3) through to ML_6 (AB_6) families, along with the ML_8 (AB_8), and ML_{12} (AB_{12}) families, featuring some specific and relatively simple illustrative worked examples.[5] Figure 5 depicts the treatment for the ML_6 (AB_6) family of *OC*-6 geometry with *TPR*-6 intermediate structures for which three pairs of doubly degenerate indices ("A", "B", and "C") were used, presumably to reflect experimental systems and reduce complexity instead of all "L atoms" being assigned distinct indices,.

Muetterties presented the transformations between different polytopal forms, called "traverses," equally as both geometry transforming operations and as real physical motions (mechanisms), though the importance of these distinctions was not addressed in detail.[5] Combinatorics and Group Theory were employed (the permutations) to indicate general principles, and Graph Theory was used to indicate pairwise relationships.

The difficulty of depicting the resulting graphs for human readability was pointed out and "stereochemical matrices" were

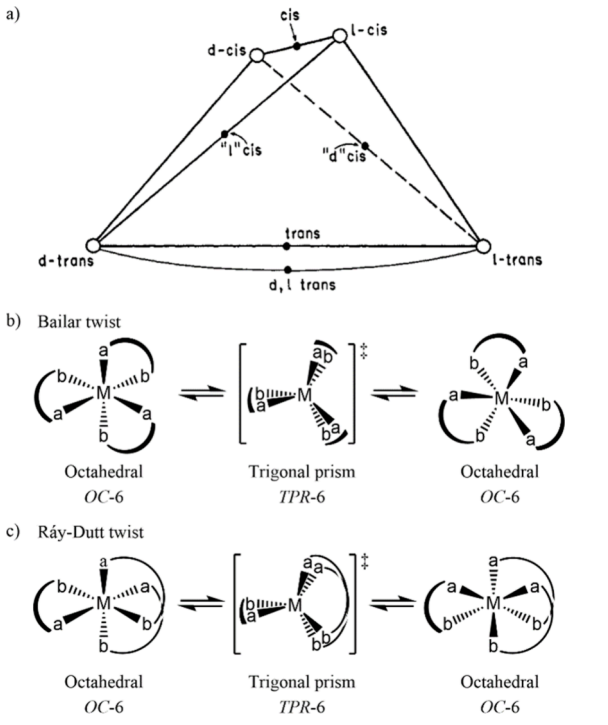

Figure 4. (a) Muetterties' graph of the topological representation of *tris* unsymmetrical-chelate *OC*-6 complexes $M(a{-}b)_3$. Reprinted from ref 3. Copyright 1968 American Chemical Society. The graph vertices shown as open circles at the vertices of the tetrahedron represent the *OC*-6 configurations while the filled circles are the *TPR*-6 intermediate structures arising through either the Bailar or Ráy-Dutt twist mechanisms. (b) Schematic diagram showing the Bailar twist mechanism. (c) Schematic diagram showing the Ráy-Dutt twist mechanism.

https://doi.org/10.1021/acsorginorgau.4c00005
ACS Org. Inorg. Au 2024, 4, 356−372

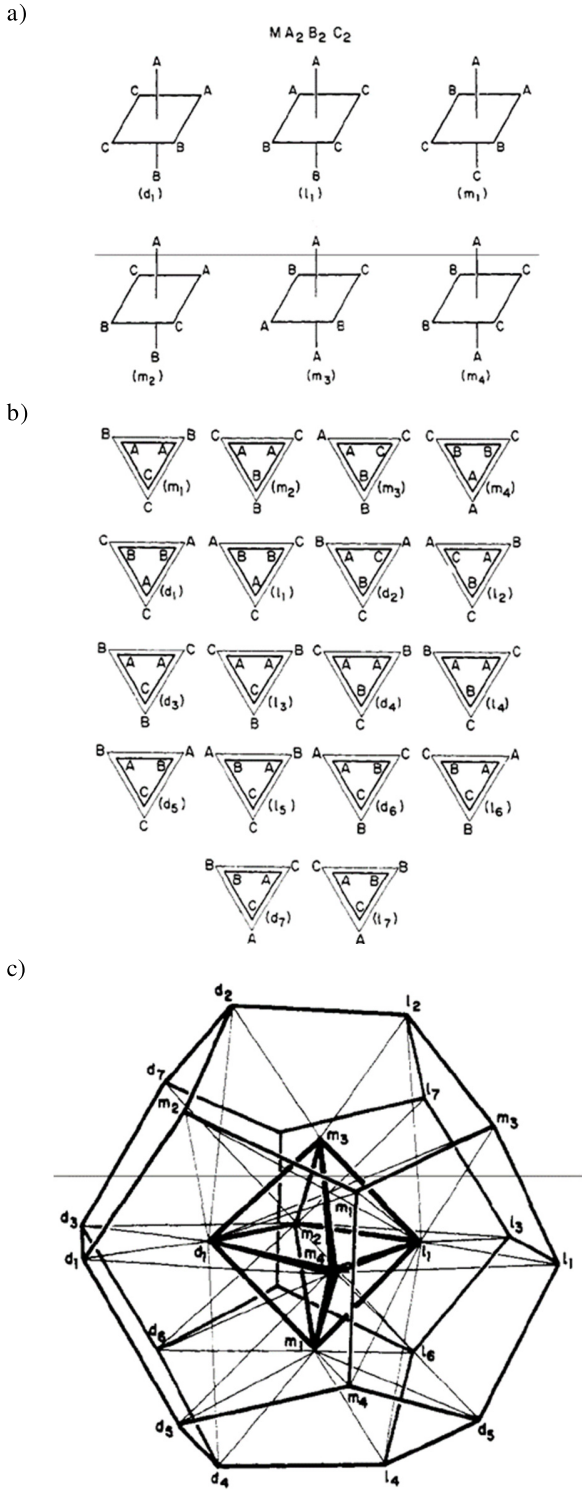

Figure 5. (a) The six distinct *OC*-6 stereoisomers of $MA_2B_2C_2$. (b) The 18 distinct *TPR*-6 stereoisomers of $MA_2B_2C_2$ as viewed from the tope face of the prism. (c) Muetterties graph of the *OC*-6 and *TPR*-6 stereoisomer relationships. The fine lines interconnecting the inner octahedrally arranged graph vertices (the *OC*-6 configurations) with the outer dodecahedrally arranged graph vertices (the *TPR*-6 configurations) are the graph edges representing single-step changes in geometry. The heavy lines only serve to indicate the layout of the graph vertices. Adapted from ref 5. Copyright 1969 American Chemical Society.

introduced to represent a graph.[5] Muetterties' stereochemical matrices give the shortest number of single concerted reaction steps needed to interconvert between two permutation stereoisomers.

The second of these seminal papers[4] focused mainly on the five atom family "ML_5" and "M_5". In this, Muetterties proposed six processes as reproduced in Figure 6, the first of which corresponds to the Berry pseudorotation mechanism (also shown in Figure 1b), with the others presented as conceptual alternatives that exhibit different ligand permutation patterns. The topological analysis began with generation of the different stereochemical matrices for the processes considered, assuming distinctly labeled ligand-atoms of the general form ML_5 = MABCDE. To provide a basis for the design of experimental systems for differentiating between mechanisms, Muetterties went on to identify five cases MA_4B, MA_3B_2, MA_2B_2C, MA_3BC, and MA_2BCD and gave their corresponding stereochemical matrices—all of which are submatrices of that for the general system MABCDE. The reasoning behind the approach was that, after accounting for electronic and steric effects, experimental rates should inversely correlate to the *number of steps* required to interconvert stereoisomers. This reasoning provided a rich

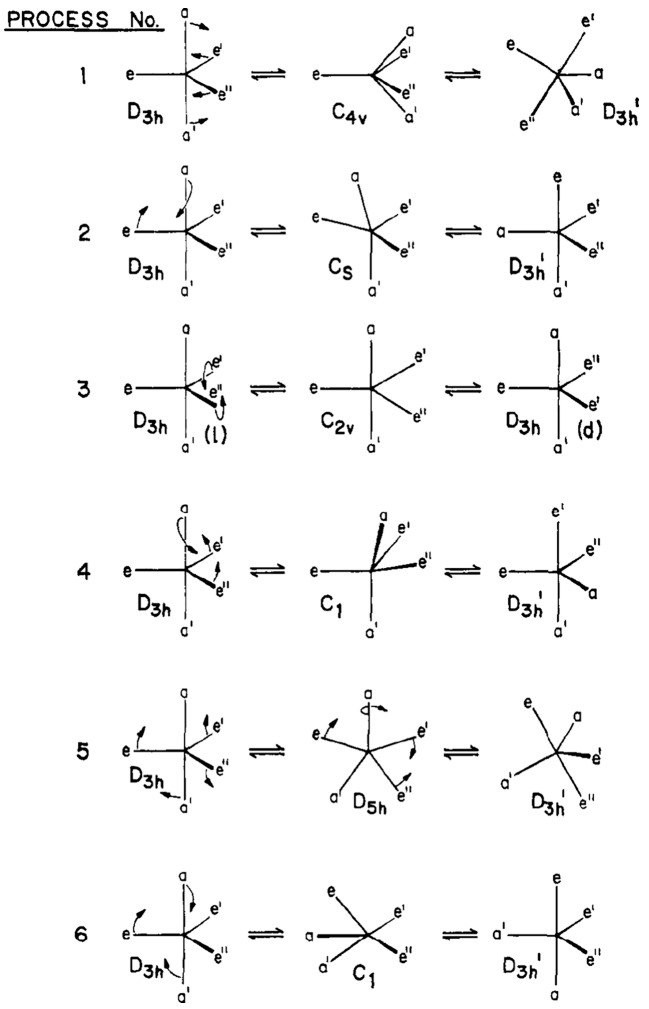

Figure 6. Muetterties' six proposed processes for interconverting *TBPY*-5 permutation stereoisomers. Process 1 is the Berry pseudorotation as shown in Figure 1b. Reprinted from ref 4. Copyright 1969 American Chemical Society.

https://doi.org/10.1021/acsorginorgau.4c00005
ACS Org. Inorg. Au 2024, 4, 356−372

source of inspiration for experiment,[25,26,42,47,67−70] some of which will be discussed later in this Perspective.

This second seminal paper[4] also examined cases incorporating one and two bidentate chelating ligands, with these imposing the restriction that, owing to steric constraints, such ligands cannot simultaneously occupy both axial positions.

Muetterties further went on to briefly describe[6] the ML_9 family considering the trigonal prism square-face tricapped structure (polytope), the square antiprism square-face monocapped structure, and an additional structure of C_{2v} symmetry. The ML_{11} family, considering polytopes of various symmetries, was also briefly described. Due to the large numbers of permutation configurations possible (hundreds of thousands in the case of ML_9), the corresponding stereochemical matrices were not given but the condition of "set closure" was discussed. Set closure in this context means that the allowed ligand position-permuting operations acting on any set member yields another member of that set. Set closure is a required aspect of any systematic chemical classification scheme.

Early Adoption of Polytopal Rearrangement Approach

The year 1970 saw five important papers published relating to the model. The first pair of papers,[7,9] by Muetterties et al., focused on the NMR determination of stereochemical nonrigidity in hexacoordinate iron hydrides of the form H_2FeL_4, where L is a phosphine ligand. Typically, hexacoordinate structures are highly thermally stable toward polytopal rearrangements, but not so in these complexes. The mechanism interconverting the different permutation stereoisomers was described as "hydride tunneling" − this language harkened back to the description of pseudorotation by Berry[84] a decade earlier in which the structural changes were described as tunneling between the two local minima of a double well potential energy surface (PES). This work was followed up by a series of three detailed papers[10,11,13] looking at fluxionality in these Fe complexes and their Ru analogs.

That same year, Shapley and Osbourne[38] reported on fluxionality in pentacoordinate transition metal complexes, specifically iridium(I) complexes. The importance of fluxionality/stereochemical nonrigidity, even in hexacoordinate complexes, would later emerge as a common, and presumably essential, property for numerous transition metal-based catalysts including those for industrially important metathesis and polymerization reactions. Indeed, Thorn and Hoffmann in 1978 reported a highly detailed analysis of polytopal rearrangements involved in olefin insertion reactions of Pt coordination complexes.[39] More recently, Kahn et al., reported[43] how a polytopal rearrangement operating on a Ru-carbene pentacoordinate complex is necessary to explain an olefin metathesis-based stereochemical "inversion" reaction. In a related setting, Tao et al. discussed polytopal rearrangements at play in Re octacoordinate hydride complexes[97]—these being exemplars of complexes useful for C−H bond activation.[64,65]

Detailed Implementation of the Polytopal Rearrangement Model

Also in 1970, an important paper by Mislow described holistically implementing the polytopal rearrangement model to comprehensively analyze rearrangements of pentacoordinate reaction intermediates arising from S_N2 reactions on quaternary phosphonium compounds.[66] The pentacoordinate intermediate species were presumed to exist for long enough to undergo Berry pseudorotation reactions. In that paper, Mislow presented the general graph for Berry pseudorotation of all 20 *TBPY*-5 "ML_5" permutation stereoisomers in which all "L atoms" are distinctly indexed.

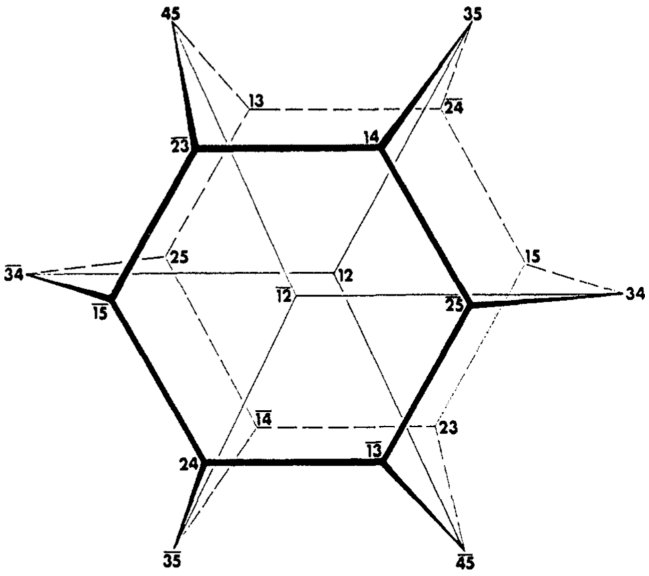

Figure 7. Mislow's representation of the Desargues-Levi graph used to describe Berry pseudorotation. Graph vertices, representing the 20 different *TBPY*-5 permutation stereoisomers, are labeled by the indices of the axial atoms. The 30 graph edges connect the different permutation stereoisomers via the Berry pseudorotation mechanism. The *SPY*-5 intermediates for the Berry pseudorotation mechanism are not shown. Reprinted from ref 66. Copyright 1970 American Chemical Society.

This graph (Figure 7) as applied to Berry pseudorotation, and identified as the "Desargues-Levi graph", was presented for the first time and in a layout that would be used by later chemistry researchers.[12,48,98] Additionally, Mislow looked at the single bidentate-chelate case "$M(L{-}L)L_3$" where two of the 20 *TBPY*-5 species (graph vertices) and six of the 30 transformations (graph edges) involving them are excluded, producing a simpler subgraph (Figure 8).[66]

As shown in Figure 8a, Mislow depicted how nucleophilic attack on either an edge or face of a tetrahedral (*T*-4) phosphonium species installed the nucleophile at either an equatorial (indicated by "**e**") or axial (indicated by "**a**") position, respectively. Similarly, a reverse reaction is feasible where a *TBPY*-5 species can eliminate a leaving group to yield a *T*-4 species. The *TBPY*-5 intermediate species in question can subsequently undergo Berry pseudorotation rearrangements along the graph edges, as shown in Figure 8b. Reactants and products enter and exit the reaction graph at the graph vertices. Mislow used molecular modeling of the species to assign relative energies to *TBPY*-5 structures (graph vertices) and activation energies for the Berry pseudorotation transformations (graph edges). Taken together, the Mislow approach demonstrates how implementing the model can account for both reaction patterns and kinetics in carefully devised chemical systems. Importantly, it suggests a one-to-one relationship between the reaction graph topology and the network of minimum energy pathways on the corresponding PES.

Turnstyle Rotation Alternative to Berry Pseudorotation

In 1971, Ugi et al.[20] introduced a new AB_5 polytopal rearrangement called the "turnstyle rotation" for permutation isomerism in *TBPY*-5 species.

https://doi.org/10.1021/acsorginorgau.4c00005
ACS Org. Inorg. Au 2024, 4, 356−372

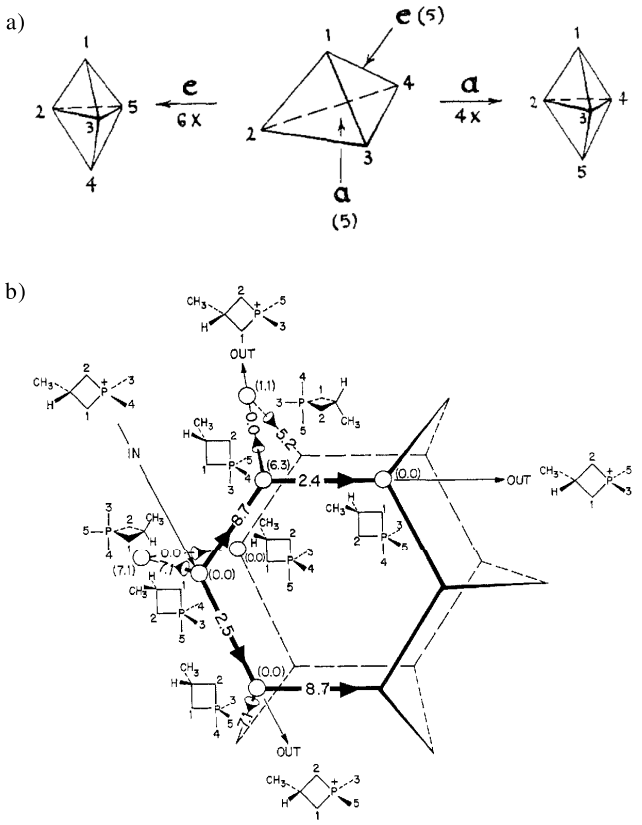

Figure 8. (a) Attack of a nucleophile on the *T*-4 species installs the nucleophile at either an equatorial or axial position depending upon whether it enters via a *T*-4 edge or face, respectively. (b) Graph for Berry pseudorotation occurring in the bidentate chelate case M(L–L)L_3 under the condition that the chelating atoms cannot simultaneously occupy both axial positions and all L atoms are distinguishable. This is a subgraph of the Desargues-Levi graph shown in Figure 7. Overlaying the graph are example structures resulting from nucleophilic attack on *T*-4 phosphonium species giving *TBPY*-5 species (the graph vertices) and select subsequent Berry pseudorotation polytopal rearrangements (the graph edges). Numbers in parentheses are calculated relative energies of *TBPY*-5 species and those along the graph edges are Berry pseudorotation minimum activation energies in the directions indicated; all values in kcal mol^{-1}. Adapted from ref 66. Copyright 1970 American Chemical Society.

This seventh mechanism (in addition to Muetterties' six as shown in Figure 6) can be thought of as Muetterties' processes 2 and 4 occurring simultaneously in counter-rotating fashion, as indicated in Figure 9.

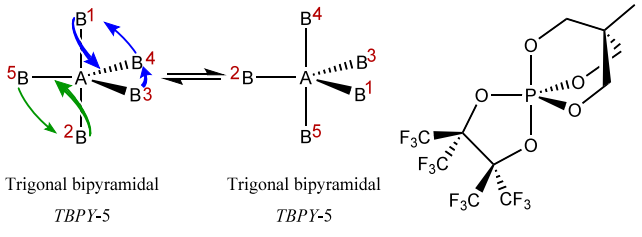

Figure 9. Turnstile rotation mechanism of Ugi et al.[20] for *TBPY*-5 AB_5 indicated as the simultaneous counter-rotation of Muetterties' processes 2 (green arrows) and 4 (blue arrows) as outlined in Figure 4. B atoms are assigned distinct indices (red) to show the permutation isomerism.

The rationale for proposing this mechanism was that, just like Berry pseudorotation, it leads to a positional exchange of the two axial and two of the three equatorial B atoms. It was argued that experimental evidence validating the Berry pseudorotation mechanism is equally consistent with turnstyle rotation. Several complexes of P featuring one bidentate ligand and one tridentate ligand were presented (e.g., that shown in Figure 9) to experimentally probe the question. This inspired much theoretical and experimental work that could distinguish between the two mechanisms[23,25,87] involving the synthesis and kinetics investigation of numerous cleverly designed chemical systems, as is discussed below.

Intrinsic Reaction Coordinate Following

In 1999, Mauksch et al. reported a theoretical analysis[31] of the seesaw-shaped (*SS*-4) SF_4 system as a model for both isoelectonic-analogues and more complex bidentate chelate systems.[99−102] This work assessed two alternative mechanisms: Berry pseudorotation, in which the lone pair on the central atom acts as a "ligand", and the "lever-mechanism", in which the lone pair undergoes significant rehybridization during the rearrangement process. An important aspect of this analysis was the use of intrinsic reaction coordinate (IRC)[103] following—a computational modeling method that generates minimum energy pathways leading energetically downhill away from a given transition-state structure (TS) and toward local minimum structures.

RECENT DEVELOPMENTS

Symmetry and Shape Measures

Early this century, the Alvarez group reported their development of continuous symmetry measure (CSM)[104] (following earlier work[105]) and continuous shape measure (CShM).[106] Both CSM and CShM are geometric parameters based upon "minimal distortion" polytopal rearrangements between idealized high-symmetry reference systems. Under the hypothesis that such minimal distortion pathways correlate with minimum *energy* pathways, much experimental X-ray structural (static geometric) information was analyzed. The CSM and CShM derived from these static structure geometries were found to correlate with the minimal distortion measures. This showed that CSM and CShM can be used to describe, within a reasonable approximation, polytopal rearrangements in real systems.

Detailed Appraisal of Polytopal Rearrangements in Pentacoordinate Systems

In 2010, Couzijn et al. (the Lammertsma group) revisited and rigorously assessed much of the previous experimental and theoretical work pertaining to AB_5 systems.[48] Noting the often subtle and complex ways that AB_5 systems change shape during a rearrangement, using curvilinear internal coordinates, they devised a robust geometrical analysis that could be *generally* applied to any *TBPY*-5 AB_5 system. Their approach relied upon a single "topology parameter" (TP) based upon internal coordinates that ranges from TP = 0, for a C_{4v} symmetric *SPY*-5 geometry, up to TP = 1, for a D_{3h} symmetric *TBPY*-5 geometry. Through density-functional theory modeling and IRC following of the experimental systems, their analyses showed that turnstile rotation in Ugi's compounds (e.g., as in Figure 7) is equivalent to the Berry pseudorotation process. Further, they showed that Muetterties' mechanisms 4 (what they designate "M2") and 2 (what they designate "M3") as shown in Figure 6 are composed

https://doi.org/10.1021/acsorginorgau.4c00005
ACS Org. Inorg. Au 2024, 4, 356−372

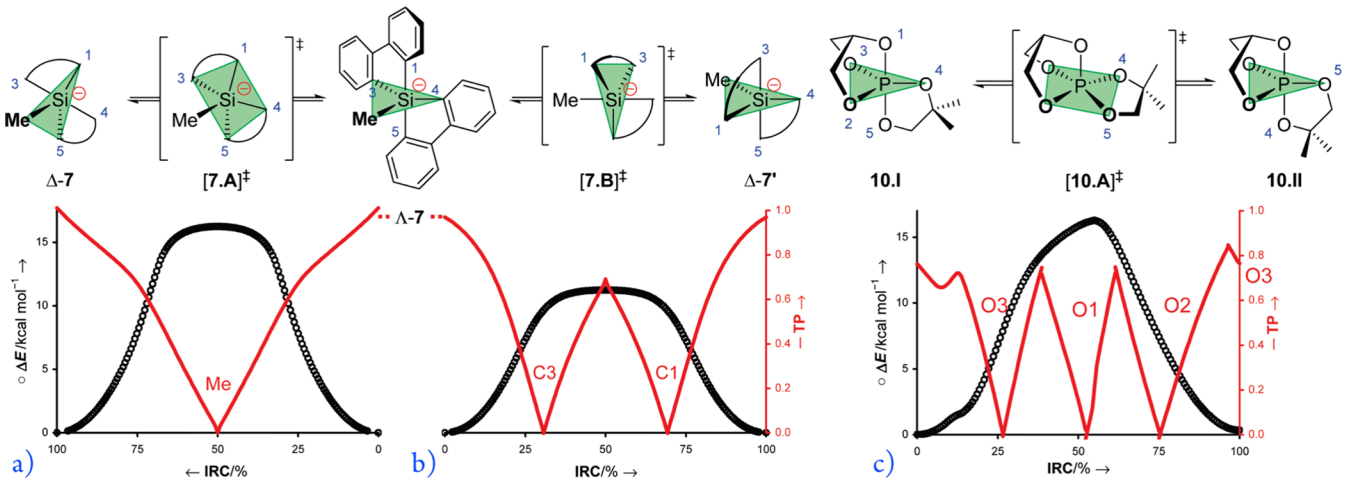

Figure 10. Results of analysis of rearrangements in *TBPY*-5 AB_5 species by the Lammertsma group. Plots of intrinsic reaction coordinate (IRC) versus topology parameter (TP) and potential energy for three experimental systems as modeled by DFT. (a) Rearrangements between **Δ**-7 and **Λ**-7 via a Berry pseudorotation mechanisms with the characteristic single "V" shape of TP. (b) Muetterties process 4 operating between **Λ**-7 and **Δ**-7′ indicating two successive Berry pseudorotations. (c) Muetterties process 2 operating between **10.I** and **10.II** indicating three Berry pseudorotation. Adapted from ref 48. Copyright 2010 American Chemical Society.

of two and three *successive* iterations of Berry pseudorotation processes, respectively.

In Figure 10a are shown the calculated[48] energy (black) and TP (red) one-dimensional paths for the Berry pseudorotation mechanism operating on the silicate system having permutation stereoisomers **Δ**-7, **Λ**-7, and **Δ**-7′. Along the IRC, the TP traces out a "V" shape—this being a characteristic of Berry pseudorotation. The corresponding analysis for process 4 (their "M2") operating on **Λ**-7 to give **Δ**-7′ is shown in Figure 10b. Here the TP makes two successive "V"s. The relatively low value of TP ≃ 0.7 at the midpoint is due to constraining effects of the chelate rings restricting access to perfect D_{3h} symmetric *TBPY*-5 geometries. The corresponding analysis of process 2 (their "M3") operating on **10.I** and **10.II** showed the TP making three successive "V"s as is shown in Figure 10c.

The use of the topology parameter and its derivation from internal coordinates thus provided a robust method of characterizing the subtle geometric changes that occur during polytopal rearrangements in pentacoordinate systems. This work by Couzijn et al.[48] stands as the centerpiece to a 2011 Highlights article by Moberg[98] where an excellent overview is given of these findings, the background inspiring it, and the implications for polytopal rearrangements in *TBPY*-5 species. (There are, however, minor labeling errors in the Desargues-Levi graph within that overview;[98] for example, graph vertex "12" should be adjacent to graph vertex "35" and not "53").

Polytopal Rearrangement in a Bicoordinate Center

In 2018 we reported the experimental demonstration of "bond-angle inversion" (now more accurately described as bond-angle *reflection*) at bicoordinate oxygen operating in a quinoxalino-porphyrin-bound *transoid* B(F)−O−B(F) complex.[1] This polytopal rearrangement at oxygen was shown to be a bent (*A*-2) geometry opening to linear (*L*-2) geometry at the TS, and then reflexing to *A*-2 as shown in Figure 11b. The lower structures and blue minimum energy pathway PES correspond to the *transoid* B(F)−O−B(F) group while the upper structures and red minimum energy pathway correspond to possible *cisoid* isomers. Note that throughout the stereoisomerization processes shown in Figure 11b, the absolute configurations of the *T*-4 B atoms are unchanging.

The emplacement of the B(F)−O−B(F) group inside the symmetry-broken porphyrin is critical for two reasons. First, the steric constraints of the porphyrin cavity restrict the motion of the O atom to a plane normal to the quasiplane of the macrocycle. The details of the changes in B−O−B geometries are shown in Figure 11a and c for *cisoid* and *transoid* structures, respectively. This steric restriction completely suppresses any competing torsion-based stereoisomerization processes to reveal a pure bond-angle reflection process. The second function of the symmetry-broken porphyrin is to make the bond-angle reflection isomers diastereomeric. In effect, the symmetry-broken porphyrin has provided an "absolute frame of reference". This is indicated in Figure 11a and b by the Cartesian axes. Consequently, the two different *orientations* (in an "internal-coordinate" sense) of the B−O−B *A*-2 polytopes translate into distinct physical and optoelectronic properties; the bond-angle reflection stereoisomers are diastereomeric. Further, the stereoisomeric differences in the stereoisomers could not be described using any existing system—indeed, **2a** and **3a** would be given the *same* name within the nomenclatural approach at that time despite these compounds being isolable, and with distinct NMR and optical properties. In response, we introduced the concept of "akamptisomerism" as the bond-angle reflection analogue of atropisomerism, along with new nomenclatural stereodescriptors.[1]

From the earliest publications pertaining to polytopal rearrangements,[5] the AB_3 system was generally considered to exhibit minimal complexity. It then followed that the simpler AB_2 system would also be simple though this was not directly addressed in any of the earlier publications.

Our work[1] demonstrated that AB_2 is not as trivial a polytopal rearrangement case as could be supposed, and that unanticipated stereoisomerism could still be discovered.

The finding of novel stereoisomerism arising in the AB_2 system led us to look at the broader subject of stereoisomerism in greater detail and to ask the question: *how do all the aspects of stereoisomerism fit together, and can they be unified under a single conceptual framework?*

https://doi.org/10.1021/acsorginorgau.4c00005
ACS Org. Inorg. Au 2024, 4, 356−372

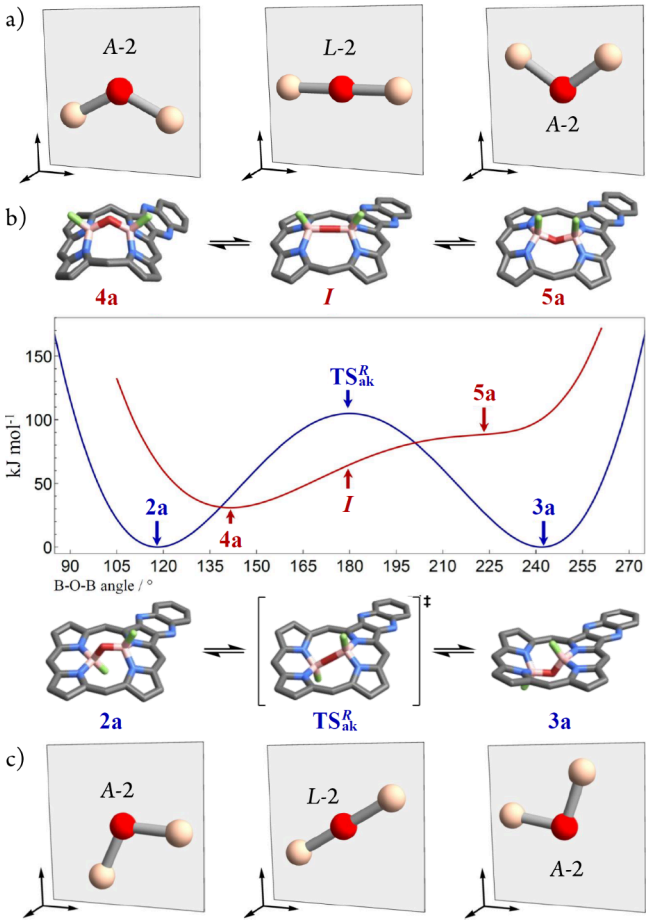

Figure 11. Bond-angle reflection polytopal rearrangement operating at a bicoordinate oxygen (central red atom) in quinoxalinoporphyrin-bound B(F)−O−B(F) complexes. (a) Detail of the B−O−B geometry changes corresponding to the anticipated *cisoid* complexes **4a** and **5a**. Atomic motions are constrained to the plane indicated and the different orientations of the *A*-2 polytope are distinguishable. (b) Upper structures and red minimum energy pathway PES for interconversion of two of four possible *cisoid* diastereomeric stereoisomers (akamptisomers) **4a** and **5a**. The lower structures are two of the four experimentally observed *transoid* stereoisomers and correspond to the blue minimum energy pathway PES. Peripheral H atoms and *meso*-substituents not shown. c) Detail of the B−O−B geometry changes corresponding to the observed *transoid* complexes **2a** and **3a**. Adapted with permission from ref 1. Copyright 2018 Springer Nature.

General Curvilinear Coordinate System

In 2020, Zou et al. (Kraka group) reported a general approach for describing polytopal rearrangements based upon the displacements of vibrational normal modes.[32] Being based upon an extension of the Cremer−Pople puckering coordinates[107] and the Zou−Izotov−Cremer deformation coordinates[108] for ring structures, their approach can be applied to arbitrary *n*-coordination (AB_n).

Briefly, their approach takes high-symmetry reference systems AB_n and makes a tabulation of the vibrational normal modes for each. There is the implicit assumption that force constants for A−B stretches are much larger than those for any B−A−B bends so that the bond-stretch modes separate out from the softer modes dominated by bond-angle changes. Armed with this tabulation, a polytopal rearrangement process can be modeled using a set of curvilinear coordinates derived from these normal-mode displacements. Multiple modes (of the same or different symmetries) can be combined using a coordinate system typical of those used in Jahn−Teller analyses yielding new curvilinear coordinates. Typically, the choice of reference structure is made based upon similarity to the TS of the real system.

This approach represents a significant improvement over prior attempts[104−106] as, *in principle*, the method is capable of spanning the full configuration space in the vicinity of the reference geometry. Different PESs can readily be obtained depending upon which modes are included in a PES scan. We posit that the inclusion of *all modes* would generate the *full* PES for the AB_n system.

Figure 12 gives the example[32] of PF_5 using the *SPY*-5 geometry (having the C_{4v} symmetry point group) as the reference AB_5 system. Figure 12a shows the two normal modes $\mathbf{I}_6$ and $\mathbf{I}_7$ that are combined as a B_4-ring deformation (t_2, τ_2) using the Jahn−Teller coordinate-system approach. In Figure 12c is the resulting 2D relaxed PES scan of (r_5, ϕ_5) corresponding to (t_2, τ_2). The horizontal blue dotted line corresponds to a Berry pseudorotation process between the two abutting D_{3h} structures.

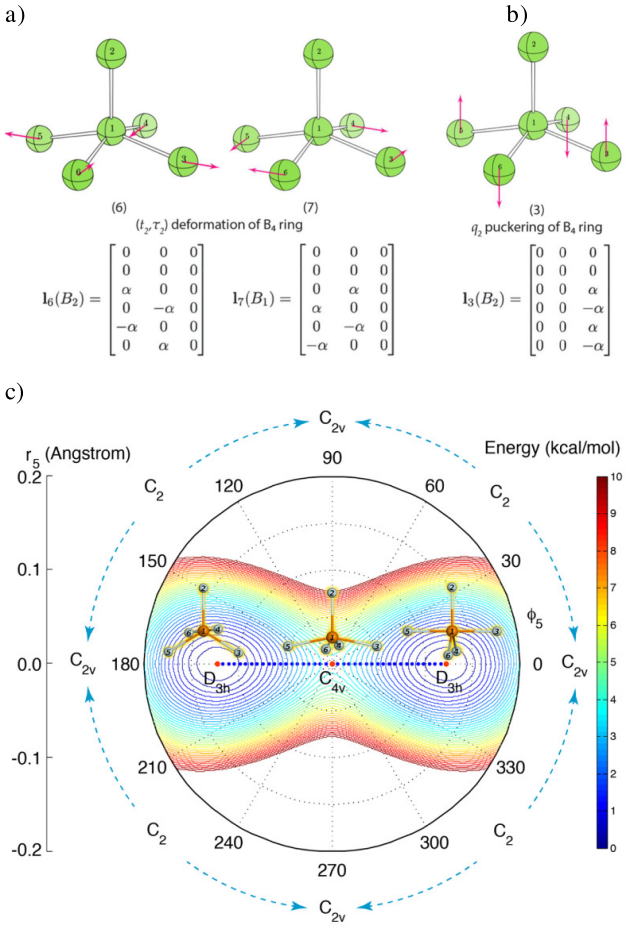

Figure 12. Implementation for PF_5 of the method of Zou et al.[32] for generating curvilinear coordinate systems for describing polytopal rearrangements in AB_n systems based upon vibrational normal modes. (a) The B_4 distortion modes $\mathbf{I}_6$ and $\mathbf{I}_7$ are combined using a Jahn−Teller approach to give (t_2, τ_2). (b) The $\mathbf{I}_3$ mode which corresponds to Berry pseudorotation. (c) The 2D PES relaxed scan of (r_5, ϕ_5) corresponding to (t_2, τ_2). The horizontal dotted blue line corresponds to a Berry pseudorotation process between the two abutting D_{3h} structures. Adapted from ref 32. Copyright 2020 American Chemical Society.

https://doi.org/10.1021/acsorginorgau.4c00005
ACS Org. Inorg. Au 2024, 4, 356−372

In PF_5 at the C_{4v} symmetric *SPY*-5 TS, the vibrational mode with the imaginary frequency corresponding to the Berry pseudorotation and labeled $\mathbf{I}_3$ in Figure 12b. This features an out-of-plane puckering of the B_4 ring. The Berry pseudorotation minimum-energy pathway that appears in Figure 12c is a consequence of the "relaxed nature" of this PES scan. Within it, the displacements manifested in mode $\mathbf{I}_6$ either stretch or compress the relatively stiff A−B (P−F) bonds, forcing out-of-plane motions. A similar (if not identical) PES would have resulted if $\mathbf{I}_3$ was used in place of $\mathbf{I}_6$ as both modes are of the same "B_2" symmetry.

Further, in that paper,[32] Zou et al. reported successful application of their method to

- SF_4 using a *T*-4 AB_4 reference system of T_d symmetry,
- $Fe(CO)_5$, a bis-bidentate silicate, a bidentate-tridentate phosphane, and IF_5 using the *SPY*-5 AB_5 reference system of C_{4v} symmetry,
- Ga(III)-tris-bidentate complexes, using the *TPR*-6 AB_6 reference system of C_{3h} symmetry, and
- IF_7, using the *PBPY*-7 AB_7 reference system of C_{5h} symmetry (this reference system corresponding to a local minimum and not a TS geometry).

While much of this work focused on the computational-chemistry implementation of their coordinate system, from our perspective, a key point is the use of vibrational normal modes as a basis for generating geometries that *span the configuration space*—a powerful general approach for generating all possible polytopal geometries for arbitrary coordination number.

Summary

The recent work discussed here features a common theme relating to the implications of an approximation explicit in the polytopal rearrangement model; that of the limited focus on high- symmetry *idealized geometries* and the presumed minimal distortion pathways connecting these.

The work of the Alvarez group showed that this approximation was reasonable in many instances with the distortions from ideal geometries tending to fall along the interconnecting minimal distortion paths. We and the Lammertsma group implemented the IRC-following technique to examine the precise geometry changes involved for the respective polytopal rearrangements examined. For our AB_2 systems, the IRC path corresponded to a simple bond angle change. The various AB_5 systems examined by the Lammertsma group required a more complex topological parameter derived from a combination of internal coordinates to assess where on the Berry pseudorotation pathways the geometries lie. In both cases, only a 1D slice through a higher dimensional PES was traced out.

The major advance comes from the recent work by the Kraka group where they introduced a technique to generate geometric configurations that, *in principle*, span the full configuration space and hence the full PES.

A MODERN CHALLENGE: COMPREHENSIVELY CLASSIFYING STEREOISOMERISM

The focus of the earliest work on the polytopal rearrangement model was only to describe permutation stereoisomers and their interconversions.[2−18,20,23,25,66,87] With this narrow focus, approximations, such as use of idealized geometries, provided a practical solution for the problems of interest at the time.

The more recent work sought to both test the validity of these approximations[31,48,104−106] and begin to probe the chemical space between them[1,31] and in their vicinity.[32,48] The formal language given in the following section is introduced to precisely and concisely describe the structure of the full configuration spaces for AB_n systems. Further, we introduce a *mathematically rigorous* treatment of the graph representation of polytopal rearrangements.

Terminology and Representation

As recently pointed out,[32] the need for a consistent and precise terminology is made clear when one wishes to search the literature wherein many synonyms, or "almost-synonyms", exist for "polytopal rearrangement" depending upon the context: "nonbond-breaking" permutation of nuclear positions for isomerization, permutation isomerization, polyhedral rearrangement/interconversion, nondissociative ligand exchange, nondissociative stereoisomerization, internal ligand exchange, intramolecular ligand exchange, stereomutation, fluxionality, topomerization, pseudorotation, pyramidal inversion, and bond-angle inversion. Indeed, Muetterties' early papers[2,3] reflect this as he struggled to find a name for the emerging conceptualization of the model. Curiously, in some of his later papers,[16,17] he retreated from using the term "polytopal rearrangement".

Polytope Definition. Within the context of the model, a polytope is defined to be the *m*-dimensional generalization of a polyhedron. Specifically, the polytope is the general shape—the "convex hull"—formed by points representing A and all the B atoms in a complex of general form AB_n. For a linear coordination center *L*-2, the polytope has one dimension and is the *line segment*. For a nonlinear molecule, where all atoms lie in a single plane, the polytopes have two dimensions and are *polygons*. Finally, for AB_n, $n \geq 3$, where A and all B are noncoplanar, the polytope has three dimensions and is a *polyhedron*. Polytopes need not be "regular" or exhibit high symmetry. This definition for polytope is approximately synonymous with the existing term "coordination polyhedron" but is more mathematically prescriptive for the general case.

Graphically Representing Polytopes. There are several different ways of graphically representing a polytope, each exhibiting strengths, and weaknesses.

Figure 13a shows bonding to a tetrahedral center as typically represented in 2D using the wedge-hash convention[109] to indicate stereochemical configuration.

In Figure 13b, only the edges (in blue) of the defining tetrahedron are indicated, making the overall structure of the polytope (the tetrahedron) the obvious feature. This "edge-only" style is only commonly used when depicting inorganic species of high coordination number, for which otherwise a multitude of radiating bonds from the center would be visually confusing. For smaller coordination numbers, this edge-only

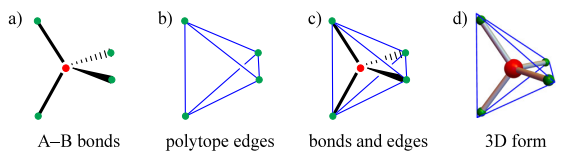

Figure 13. Equivalent representations of the tetrahedral polytope. (a) Typical 2D representation using the wedge-hash convention[110] with only the A−B bonds shown. (b) Representation showing only the edges of the polytope. (c) Representation combining both (a) and (b). (d) 3D representation of (c). The red dots and sphere represent the central atom "A", and the green dots and spheres represent the ligating atoms "B".

https://doi.org/10.1021/acsorginorgau.4c00005
ACS Org. Inorg. Au 2024, 4, 356−372

approach can lead to a different type of ambiguity, for example, where in the case of a "square planar" polytope, it could be mistaken for cyclobutane.

In Figure 13c, both styles are combined with distinct colors differentiating the respective bond and edge features. Figure 13d shows a more realistic rendering of Figure 13c with the 3D visual cues helping to make the spatial relationships clearer. In the interests of using a consistent convention fit for *any* coordination number and orientation, this is our preferred style. A tool for generating these images is provided in the Supporting Information of this Perspective.

Taxonomic Hierarchy. There is an important distinction to be made between the *general shape* of a polytope and when that same shape has a specific arrangement (configuration) of *distinct* indices assigned to the polytope vertices.

When discussing *only* the shape, the polytope is referred to as a polytope *genus* (plural: *genera*; adjectival form: *generic*); for example, Figure 14b shows the tetrahedral genus and its nomenclatural polyhedral symbol *T*-4 as listed in the IUPAC "Red Book",[111] section IR-9.3.2. Such polyhedral symbols are well established and sometimes used when describing coordination geometries in the context of the VSEPR model. As with Muetterties' original description, the *T*-4 genus belongs to the AB_4 *family* (Figure 14a) (plural: *families*; adjectival form: *familial*).

When distinct vertex indices are specifically assigned, the polytope is referred to as a polytope *species* (plural: *species*; adjectival form: *specific*). Figure 14c shows the two different ways of assigning distinct indices to a tetrahedron. If the indices are used in the same way as the Cahn-Ingold-Prelog (CIP) priorities,[112] then the adaption of chemical nomenclatural *T*-4-*S* and *T*-4-*R* polyhedral configuration or absolute configuration symbols (IUPAC "Red Book",[111] sections IR.9.3.3 and IR.9.3.4, respectively) can be assigned for each species, providing a convenient and unique labeling.

This *family*−*genus*−*species* hierarchical categorization provides a structured taxonomic system applicable for all scenarios. As an example, although the *T*-4-*S* species has C_1 symmetry (the distinct indices break the symmetry), it belongs to the *T*-4 genus and thus has T_d *generic symmetry*.

In Figure 5a are shown the six *OC*-6 stereoisomeric species of $MA_2B_2C_2$. All six species exhibit O_h generic symmetry.

Stereoisomers d_1 and l_1 have C_3 specific symmetry, with the remaining four stereoisomers, m_1−m_4, all exhibiting C_s specific symmetry.

Naming Processes. The central concept underpinning polytopal-rearrangement-mediated stereoisomerization is that of a unimolecular structural rearrangement without the formation or breaking of bonds. We call this a *stereotropic* rearrangement (Ancient Greek *στερεός* − stereós, "solid" + *τροπικός* − tropikós, "of or pertaining to a change". This is in contrast to a *desmotropic* rearrangement as characterized by changes in bonding (constitutional isomerization). This central concept is further refined by considering the *concerted* case that represents a fundamental reaction element of the polytopal rearrangement model. To encapsulate all these concepts, we introduce the symbol "R^c_{st} 1" which has been devised in an analogous manner to S_N2, E1, etc. R^c_{st} 1 is read as "rearrangement, concerted, stereotropic, unimolecular".

All polytopal rearrangements are composed of one or more successive R^c_{st} 1 processes. Further, R^c_{st} 1 can be used to refer to a real chemical process or simply a conceptual geometric change. The transformations between the species in Figures 10 and 11 are all R^c_{st} 1 processes. Later, the material relating to Figures 15 and 16 further demonstrate this point in action.

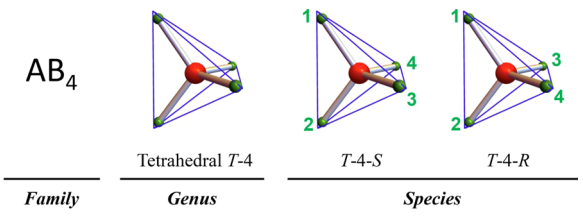

Figure 14. Distinctions between the polytope *family*, *genus*, and *species* concepts. (a) AB_4 is the polytope *family*. (b) The tetrahedral *genus* *T*-4 only refers to the general shape. (c) The two distinct ways of indexing the vertices correspond to distinct polytope *species*. Chemical nomenclatural *T*-4-*S* and *T*-4-*R* polyhedral absolute configuration symbols[111] are assigned to each species using the vertex indices to represent CIP priorities.

Naming Polytope Species

In as far as its applicability to coordination centers, the needs of chemical nomenclature closely parallel the need for descriptors of polytope species. Just as we and the Alvarez group[104,106] have used IUPAC nomenclatural polyhedral symbols to name polytope *genera* (for example, *T*-4 and *TBPY*-5), we recommend using the IUPAC nomenclatural "polyhedral configuration" and "polyhedral absolute configuration" symbols as outlined in the "Red Book"[111] sections IR.9.3.3 and IR.9.3.4, respectively, to name the polytope *species*. Unlike naming chemical compounds where polyhedral symbols need only *approximately* describe the geometry of a coordination center, when naming polytopes generic symmetries will differentiate between similar forms. Consequently, for such an approach to be fully general when used to rigorously describe polytopal rearrangements, the existing nomenclatural symbols need to be augmented with additional symbols devised in an analogous manner. While being somewhat less compact in some circumstances, this does provide the added benefit of integrating with existing chemistry software.

We have already shown an example of the two distinct *T*-4-*S* and *T*-4-*R* species in Figure 14c. In Figure 15a, we show a pair of *TBPY*-5 enantiomers annotated by their IUPAC polyhedral absolute configuration symbols. Also shown in the Figure 15a are the different symbols have been used to describe such species in the past, and those used by Muetterties,[4] Mislow,[66] Couzijn,[48] and Moberg.[98] An advantage of the polyhedral configurational symbols is their generality. Also given in the figure is an abbreviated version of the polyhedral configuration symbols in which, for example, *TBPY*-5-45-*C* becomes 45-*C*. In Figure 15b, these abbreviated symbols have been applied to all 20 graph vertices of Mislow's[66] depiction of the Desargue-Levi graph and in Figure 15c, the full nomenclatural labels are used.

Graphs, Chemical Reactions, Configurations Spaces, and Potential Energy Surfaces

As mentioned earlier, graphs are mathematical constructs that are *abstract objects*. How one represents a graph will depend upon the intent behind doing so. Mislow's representation of the Desargues-Levi graph,[66] as shown in Figure 7 and again in Figure 15b but with different nomenclatural graph-vertex labels, is a 2D projection of this graph laid out symmetrically in 3D. This makes for a particularly human-readable format and neatly places enantiomer pairs diametrically opposite one another about the graph's "center of inversion". That a graph can be represented

https://doi.org/10.1021/acsorginorgau.4c00005
ACS Org. Inorg. Au 2024, 4, 356−372

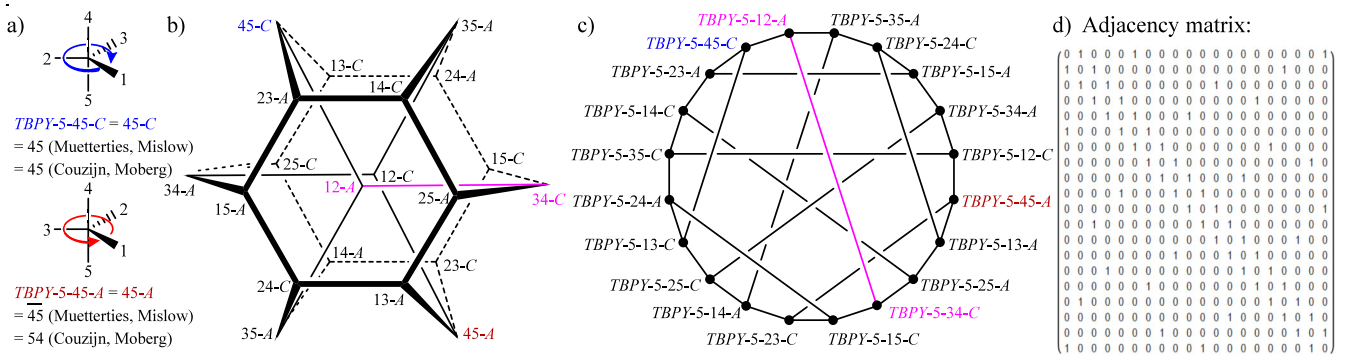

Figure 15. Equivalent representations of the Desargues-Levi graph indicating Berry pseudorotation R^c_{st} 1 processes interconnecting all 20 *TBPY*-5 species. (a) IUPAC nomenclatural absolute configuration labels (color) for species are fully general (when augmented) for any coordination number and geometry. Equivalence of compact labels of different authors are indicated. (b) Mislow's layout of the Desargues-Levi graph[68] using label format given in (a). Enantiomers, e.g., those in blue and red corresponding to species in (a), are positioned diametrically opposite the inversion center for this graph layout making for ease of human readability. Layouts like this are not a *general* possibility. (c) Circular layout of the Desargues-Levi graph.[114] Circular layouts are always possible. (d) Adjacency matrix for the Desargues-Levi graph[114] with vertex ordering corresponding to (c). Graph representations as adjacency matrices are *computer processable*.

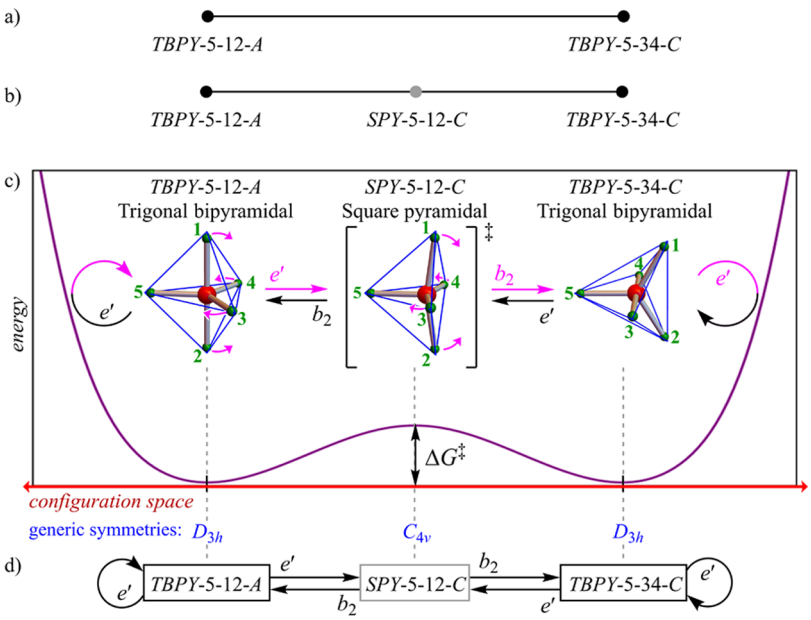

Figure 16. Stereotropic chemical reaction, graph, vibrational mode generic symmetries, configuration space, and potential energy surface relationships. (a) Undirected graph edge between Berry pseudorotation-related species *TBPY*-5-12-*A* and *TBPY*-5-34-*C*. (b) Modification of (a) with the explicit inclusion of the *SPY*-5-12-*C* Berry pseudorotation intermediate. (c) Pictorial representation of this Berry pseudorotation process showing structures corresponding to (b) overlying the one-dimensional slice through the PES from Figure 15c (purple) plotted against the configuration space (red). The transformation arrows double as directed graph edges and are labeled by their generic symmetries. Self-loops at the left and right ends correspond to the steep walls of the surface. (d) Symmetry labeled directed graph representation of (b) and (c).

neatly as such, however, is not a general possibility. Figure 15c shows a different representation of the same graph where the labeled graph vertices are now laid out in a circle.[112] Graph layouts in 2D like this are *always* possible, but become unwieldy as the number of arbitrary choices increases with graph vertex number *N*.

A computationally useful way of representing this same graph is as an *adjacency matrix*, as shown in Figure 15d.[112] Each element m_{ij} of the $N \times N$ adjacency matrix for an *N*-vertex graph is either 1, indicating vertices *i* and *j* are immediately connected ("adjacent"), or 0 otherwise.

The adjacency matrix in Figure 15d has the vertices ordered as they appear in the circle layout in Figure 15c. Adjacency matrices of undirected graphs are square and symmetric. As Muetterties noted,[5] the graphs that the polytopal rearrangement model generates, in general, are too complex for manual processing. Graph Theory is both a relatively evolved subject and an extremely active area of research,[113] owing to its wide applicability to challenges facing the modern world. Many Graph-Theoretic computational tools exist for processing graph-based data.[114−120] The representation, in general, of a graph as an *object for computation* serves to emphasize that the full power of the model will only be realized through computational means. Thus far, apart from Figure 4, all the graphs presented have been undirected graphs and only included permutation stereoisomers as the graph vertices. Notably, the intermediate polytopal forms such as TSs, have been omitted; in these examples a graph edge only represents a R^c_{st} 1 reaction/process between a reactant and a

https://doi.org/10.1021/acsorginorgau.4c00005
ACS Org. Inorg. Au 2024, 4, 356−372

product, and only *implicitly* encodes the mechanism. Despite previous limitations, it is straightforward to explicitly include intermediate forms such as a TS.[112]

In Figure 16, we show the way in which intermediate forms are included. Figure 16a depicts the undirected R^c_{st} 1 transformation of *TBPY*-5-12-*A* to *TBPY*-5-34-*C* via a Berry pseudorotation R^c_{st} 1 mechanism that corresponds to the magenta-colored edge on the Desargues-Levi graphs shown in Figure 15b and c. In Figure 16b, this graph edge is modified with the inclusion of the corresponding Berry pseudorotation TS polytopal form *SPY*-5-12-*C*.

This incorporation of an additional geometry along the reaction path begins to "fill in" the description of the chemical space between the reactant and product.

A familiar way of depicting a chemical reaction is as a minimum energy pathway along a PES (for example, Figures 10−12). In Figure 16c is shown a one-dimensional slice through the PES from 15c, giving a double well. The transformation between the two *TBPY*-5 species (local minima) via the *SPY*-5 intermediate (central local maximum) corresponds to the R^c_{st} 1 processes represented by Figure 16b. The principle that such a reaction between these three species corresponds to the curvilinear vibrational atomic displacements (shown as curved vectors at each B atom) at those precise configurations, means we can associate the generic symmetries of each respective vibrational mode with the forward and reverse reaction arrows at those points along the trajectory through the configuration space. Atomic displacements for a vibration, however, have two directions. Consequently, rigorous treatment must also include those motions that, here, correspond to the steep side walls of the PES. These reaction arrows are shown as "self-looped" arrows. While accounting for both directions of the vibrational atom displacements, this treatment "blocks" the high energy pathways that would lead to, for example, bond breaking (constitutional isomerization) and in so doing, keeps the description in the domain of stereoisomerism.

The reaction arrows in Figure 16c can now be interpreted as a *directed graph*, as shown in Figure 16d. Directed graphs, as the name implies, portray *directional pairwise relationships* between graph vertices with the directed graph edges depicted as arrows (including the self-loop arrows). For a polytopal rearrangement, the annotations to the directed edges in such a graph encode the symmetries of the vibrational atomic displacements that are "congruent" ("coinciding exactly when superimposed") with the atomic motions *at that point* on the reaction path.

Explicit in most PES presentations is a reaction coordinate against which the energy is plotted. A reaction coordinate represents a trajectory through the full *configuration space* that describes all possible geometries for the chemical system. The space spanned by the normal vibrational mode based curvilinear coordinate systems of Zou et al.[32] to describe polytopal rearrangements corresponds to such a configuration space.

The wider utility of this directed graph representation of a polytopal rearrangement is to rigorously represent, and thus encode, all the symmetry and relational information, account for both directions of all contributing vibrational modes, delineate the "boundaries" of the configuration space (e.g., the domain of stereoisomerism), and depict the topology or connectedness/shape of the corresponding PES.

A feature of this approach is that a continuum of structures all exhibiting the *same generic symmetry* can be represented by a single polytope species. This is key to our aim of classifying all polytopes as it allows for a configuration space composed of *infinite* points (the configurations) to be represented by a *finite* number of polytopes (graph vertices) and neighbor relationships (graph edges). The resulting graph is, in effect, *a structural roadmap of the corresponding configuration space*.

Typically, this structural roadmap can be used to describe isomers, transition states, etc. of AB_n. In this case, the set of polytopes provides, in itself, a finite representation of all chemically distinct molecular shapes that the entire configuration space could support. This then forms a basis for the naming and cataloguing of chemical species. The resulting graph features all possible polytopes (graph vertices) and associated R^c_{st} 1 reactions (graph edges).

It is, however, conceivable that more than one chemically distinct species manifests within a generic-symmetry contiguous region of the configuration space attributed to a single polytope. In these cases, the graph can simply be expanded to include the manifested novel chemical features, retaining a finite graph representation. Hence any possible chemical structure, no matter how unusual, can be represented using a finite polytopal-based set.

OUTLOOK

Although the polytopal rearrangement model of stereoisomerization was originally only intended to describe and account for the thermally facile interconversion of permutation stereoisomers, a careful examination of its underlying mathematical and physical principles has revealed the potential for a more general application.

Following recent work, particularly that by the Kraka group,[32] we anticipate that a vibrational normal mode based method can be exhaustively applied to generate the full stereoisomerism "configuration space" for an arbitrary coordination center AB_n. The configuration space is the m-dimensional coordinate space created by combining m vibrational modes. For AB_2, $m = 2$; and for AB_n with $n \geq 3$, $m = 2n - 3$. Additionally, such a configuration space (and subspaces thereof) can be represented by a finite graph that encodes the generic symmetries and symmetry relationships between the parts.

AB_n configuration-space graphs have two obvious applications: (i) as there is a one-to-one relationship between a graph and the corresponding PES, the topology of the graph matches the topology of the PES; and (ii) the finite and structured nature of the graph allows for a classification/categorization of the constituent configurations. It is this latter point that we anticipate providing a major contribution toward a complete and systematic description of all stereoisomerism.

To understand what a complete and systematic description of all stereoisomerism looks like, we must examine some of the fundamentals of molecular structure and how it relates to stereoisomerism.

The atom-bond-centric picture of molecular systems is long established and implicitly understood by chemists. This picture views any molecular system as a set of connected coordination centers, with each center and each chemical bond exhibiting characteristic approximate or precise geometries and dynamical behaviors. Note that, in this context, a "coordination center" just means an atom in a molecule to which two or more additional atoms are bonded. Such a picture is the basis for internal coordinate definitions of molecular geometries as frequently used in molecular modeling.

While some well-known stereoisomerism-related concepts like enantiomerism (chirality) and diastereomerism are dependent upon *global* properties of a molecule, most other aspects of

https://doi.org/10.1021/acsorginorgau.4c00005
ACS Org. Inorg. Au 2024, 4, 356−372

stereoisomerism are viewed through the lens of the atom-bond-centric picture. For example, a saturated C atom is assumed to be approximately tetrahedral, and single bonds typically are attributed low barriers to torsional motion whereas formal double bonds have typically higher barriers giving rise to isolable *E*/*Z*-stereoisomers at ambient temperatures.

Significantly, much stereoisomerism-related systematic nomenclature is heavily reliant upon this atom-bond-centric picture of molecules—the stereoisomerism for an entire molecule is given by describing the stereoisomerism of its parts and those global properties emerge from all the parts taken together.

Simple examples illustrating some features and challenges of stereoisomerism are shown in Figure 17. In Figure 17a and b, MeNHF is represented as a tetracoordinate center (C) bonded to a tricoordinate center (N). The single coordinate F and H atoms are not considered coordinate centers here. In Figure 17a is shown three different stereoisomeric species that relate to each other only by proper bond torsion differences along the C−N bond. The absolute configuration symbols for C and N remain the same for each species. In Figure 17b are three stereoisomeric species that differ in the polytopes at N. Shown as a polytopal *rearrangement*, the *TPY*-3-*R* → *TP*-3 → *TPY*-3-*S* configurational changes occur at N, leaving the rest of the molecule unchanged. Even though this is shown as a real chemical reaction, for the purposes of *classification* only the geometrical differences—the *different polytopes* — are important. Processes like those shown in Figure 17a and b can occur simultaneously.

There are complexities beyond what the examples in Figure 17a and 17 may suggest. One of these complexities is demonstrated in the example of Me−Hg−Me as shown in Figure 17c. The geometry at the Hg-atom is linear (*L*-2). Any proper bond torsion involving a *L*-2 polytope is *undefined* (a mathematical singularity) hence any general approach must be able to accommodate such a challenge.

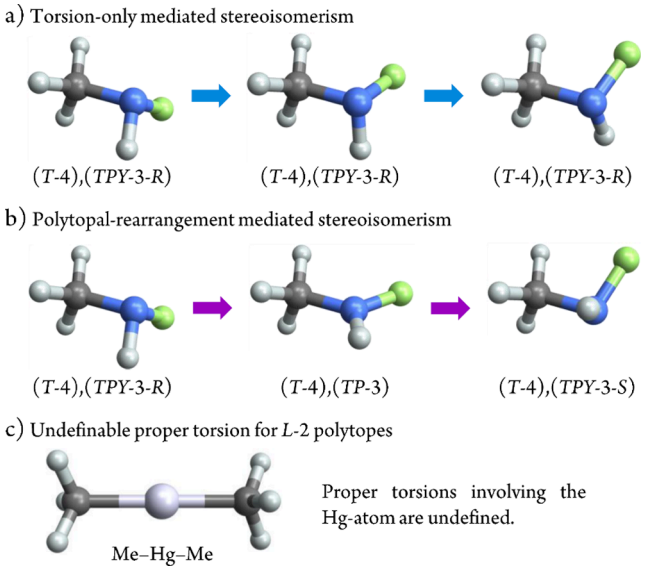

Figure 17. Simple stereoisomerism examples. (a) For MeNHF with the C (dark gray) and N (blue) coordination centers labeled by their nomenclatural polyhedral configuration symbols, two successive C−N bond torsions gives new stereoisomeric structures without effecting the configurations at C and N. (b) Polytopal rearrangement whereby the configuration at N changes from *TPY*-3-*R* → *TP*-3 → *TPY*-3-*S* without other changes in the molecule. Polytopes *TPY*-3-*R* and *TPY*-3-*S* are permutation stereoisomers at N and *TP*-3 is an intermediate. (c) $HgMe_2$ is linear (*L*-2) at Hg. The proper bond torsion at the Hg-atom is undefined.

With the mathematics for describing proper bond torsional differences appearing simple, the need for a comprehensive classification of the polytopal forms is needed. We contend that this can now be devised. Beyond this, we note that, even though polytope ideas have been explicitly delineated in application to stereoisomerism, practical applications, and even IUPAC definitions, also embrace constitutional isomerism. Therefore, a fully general polytope-based description of isomerism more broadly may be possible.

Chemistry is one of the most practical sciences as it plays a central role in our interactions with the world. From a research and technology perspective, chemists "explore chemical space" in the effort to understand, innovate, and create. Thus, far, our exploration of chemical space has revealed so much that it has resulted in the world's largest human-curated database: the Chemical Abstracts Service database.[121] Notwithstanding, our exploration has only just begun and there is now the expectation that machine-led approaches will dominate future discoveries. A complete system of stereoisomerism moves us one step closer to comprehensively defining chemical space. Such further development of this comprehensive map will greatly empower future endeavors.

■ ASSOCIATED CONTENT

Data Availability Statement

No new data were generated or analyzed in support of this study.

Supporting Information

The Supporting Information is available free of charge at https://pubs.acs.org/doi/10.1021/acsorginorgau.4c00005.

Stand-alone Wolfram Mathematica computable document format (CDF, using the free Wolfram Player https://www.wolfram.com/player/) app for generating 3D polytope models (ZIP)

■ AUTHOR INFORMATION

Corresponding Authors

Peter J. Canfield − *School of Chemistry, The University of Sydney, NSW 2006, Australia;* orcid.org/0000-0002-4974-0638; Email: peter.canfield@sydney.edu.au

Jeffrey R. Reimers − *International Center for Quantum and Molecular Structures and the School of Physics, Shanghai University, Shanghai 200444, China; School of Mathematical and Physical Sciences, University of Technology Sydney, Sydney, NSW 2007, Australia;* orcid.org/0000-0001-5157-7422; Email: jeffrey.reimers@uts.edu.au

Maxwell J. Crossley − *School of Chemistry, The University of Sydney, NSW 2006, Australia;* orcid.org/0000-0001-9851-033X; Email: maxwell.crossley@sydney.edu.au

Complete contact information is available at: https://pubs.acs.org/10.1021/acsorginorgau.4c00005

Author Contributions

The manuscript was written through contributions of all authors. CRediT: **Peter J. Canfield** conceptualization, formal analysis, methodology, software, writing-original draft, writing-review & editing; **Jeffrey R. Reimers** conceptualization, formal analysis, methodology, software, validation, writing-review &

https://doi.org/10.1021/acsorginorgau.4c00005
ACS Org. Inorg. Au 2024, 4, 356−372

editing; **Maxwell John Crossley** conceptualization, investigation, resources, supervision, validation, writing-review & editing.

Funding

Research Training Program Stipend (SC1999), the Australian Research Council grants DP0666378, DP0773847, and DP150103137, the National Natural Science Foundation of China (NSFC; Grant No. 11674212), and the Shanghai High-End Foreign Experts Grant.

Notes

The authors declare no competing financial interest.

■ ABBREVIATIONS

A-2, angular bicoordinate; CShM, continuous shape measure; CSM, continuous symmetry measure; IRC, internal reaction coordinate; *L*-2, linear bicoordinate; *OC*-6, octohedral hexacoordinate; PES, potential-energy surface; R^{c}_{st} 1, rearrangement concerted stereotropic unimolecular; *SPY*-5, square pyramidal pentacoordinate; *T*-4, tetrahedral tetracoordinate; *TBP*-5, trigonal bipyramidal pentacoordinate; TP, topological parameter; *TP*-3, trigonal planar tricoordinate; *TPR*-6, trigonal prismatic hexacoordinate; *TPY*-3, trigonal pyramidal tricoordinate; TS, transition-state structure

■ REFERENCES

(1) Canfield, P. J.; Blake, I. M.; Cai, Z.-L.; Luck, I. J.; Krausz, E.; Kobayashi, R.; Reimers, J. R.; Crossley, M. J. A New Fundamental Type of Conformational Isomerism. *Nat. Chem.* **2018**, *10*, 615−624.

(2) Muetterties, E. L. Intramolecular Racemization Processes in Pentacoordinate Structures. *Inorg. Chem.* **1967**, *6*, 635−638.

(3) Muetterties, E. L. Intramolecular Rearrangement of Six-Coordinate Structures. *J. Am. Chem. Soc.* **1968**, *90*, 5097−5102.

(4) Muetterties, E. L. Topological Representation of Stereoisomerism. II. The Five-Atom Family. *J. Am. Chem. Soc.* **1969**, *91*, 4115−22.

(5) Muetterties, E. L. Topological Representation of Stereoisomerism. I. Polytopal Rearrangements. *J. Am. Chem. Soc.* **1969**, *91*, 1636−43.

(6) Muetterties, E. L.; Storr, A. T. Topological Analysis of Polytopal Rearrangements. Sufficient Conditions for Closure. *J. Am. Chem. Soc.* **1969**, *91*, 3098−9.

(7) Meakin, P.; Guggenberger, L. J.; Jesson, J. P.; Gerlach, D. H.; Tebbe, F. N.; Peet, W. G.; Muetterties, E. L. Structure and Stereochemical Nonrigidity of Six-Coordinate Complexes. *J. Am. Chem. Soc.* **1970**, *92*, 3482−4.

(8) Muetterties, E. L. Stereochemically Nonrigid Structures. *Acc. Chem. Res.* **1970**, *3*, 266−273.

(9) Tebbe, F. N.; Meakin, P.; Jesson, J. P.; Muetterties, E. L. Stereochemically Nonrigid Six-Coordinate Hydrides. *J. Am. Chem. Soc.* **1970**, *92*, 1068−1070.

(10) Jesson, J. P.; Meakin, P.; Muetterties, E. L.; Tebbe, F. N. Stereochemically Nonrigid Six-Coordinate Molecules. I. Detailed Mechanistic Analysis for the Molecule $FeH_2[P(OC_2H_5)_3]_4$. *J. Am. Chem. Soc.* **1971**, *93*, 4701−4709.

(11) Gerlach, D. H.; Peet, W. G.; Muetterties, E. L. Stereochemically Nonrigid Six-coordinate Molecules. II. Preparations and Reactions of *tetrakis*(organophosphorus)metal Dihydride Complexes. *J. Am. Chem. Soc.* **1972**, *94*, 4545−4549.

(12) Meakin, P.; Muetterties, E. L.; Jesson, J. P. Intramolecular Rearrangement Mechanisms in Five-Coordinate Complexes. *J. Am. Chem. Soc.* **1972**, *94*, 5271−5285.

(13) Meakin, P.; Muetterties, E. L.; Jesson, J. P. Stereochemically Nonrigid Six-Coordinate Molecules.' III. The Temperature-Dependent ^{1}H and ^{31}P Nuclear Magnetic Resonance Spectra of Some Iron and Ruthenium Dihydrides. *J. Am. Chem. Soc.* **1973**, *95*, 75−88.

(14) Muetterties, E. L.; Wiersema, R. J.; Hawthorne, M. F. Detection of Polytopal Isomers in the Solution State. I. Eight-Atom Family. *J. Am. Chem. Soc.* **1973**, *95*, 7520−2.

(15) Muetterties, E. L. Polytopal Form and Isomerism. *Tetrahedron* **1974**, *30*, 1595−604.

(16) Muetterties, E. L.; Guggenberger, L. J. Idealized Polytopal Forms. Description of Real Molecules Referenced to Idealized Polygons or Polyhedra in Geometric Reaction Path Form. *J. Am. Chem. Soc.* **1974**, *96*, 1748−56.

(17) Guggenberger, L. J.; Muetterties, E. L. Reaction Path Analysis. 2. The Nine-Atom Family. *J. Am. Chem. Soc.* **1976**, *98*, 7221−5.

(18) Hoffmann, R.; Beier, B. F.; Muetterties, E. L.; Rossi, A. R. Seven-Coordination. A Molecular Orbital Exploration of Structure, Stereochemistry, and Reaction Dynamics. *Inorg. Chem.* **1977**, *16*, 511−22.

(19) le Bel, J. A. Derivatives of Ammonium Chloride. *C. R. Hebd. Seances Acad. Sci.* **1890**, *110*, 144−147.

(20) Ugi, I.; Marquarding, D.; Klusacek, H.; Gillespie, P.; Ramirez, F. Berry Pseudorotation and Turnstile Rotation. *Acc. Chem. Res.* **1971**, *4*, 288−296.

(21) Bartell, L. S.; Plato, V. Gillespie-Nyholm Aspects of Force fields. I. Points-on-a-Sphere and Extended Hueckel Molecular Orbital Analyses of Trigonal Bipyramids. *J. Am. Chem. Soc.* **1973**, *95*, 3097−3104.

(22) Strich, A.; Veillard, A. Electronic Structure of Phosphorus Pentafluoride and Polytopal Rearrangement in Phosphoranes. *J. Am. Chem. Soc.* **1973**, *95*, 5574−5581.

(23) Eisenhut, M.; Mitchell, H. L.; Traficante, D. D.; Kaufman, R. J.; Deutch, J. M.; Whitesides, G. M. Pseudorotation in XPF_4. *J. Am. Chem. Soc.* **1974**, *96*, 5385−5397.

(24) Westheimer, F. H. Essay 10 - The Polytopal Rearrangement at Phosphorus. In *Organic Chemistry: A Series of Monographs*; de Mayo, P., Ed.; Academic Press: 1980; Vol. *42*, pp 229−271.

(25) Whitesides, G. M.; Eisenhut, M.; Bunting, W. M. Pseudorotation in Aryl*bis*(4,4′-dimethyl-2,2′-biphenylylene)phosphoranes. *J. Am. Chem. Soc.* **1974**, *96*, 5398−5407.

(26) Mesch, K. A.; Quin, L. D. *Syn* to *anti* Isomerization and Degradation of Phosphines of the 7-Phosphanorbornene System by Action of Methanol. *Tetrahedron Lett.* **1980**, *21*, 4791−4794.

(27) Minkin, V. I. Stereochemical and Mechanistic Consequences of the Polarity Rule and Polytopic Rearrangements in Three-coordinate Structures of Group VI Elements. *Zh. Org. Khim.* **1977**, *13*, 1129−1137.

(28) Kharabaev, N. N.; Minkin, V. I. Theoretical Modeling of the Stereoisomerization of Tetracoordinated Be(II) *bis*(Chelate) Complexes. *Russian Journal of Coordination Chemistry* **2003**, *29*, 525−528.

(29) Minkin, V. I.; Nivorozhkin, L. E.; Korobov, M. S. Stereodynamics and Degenerate Ligand Exchange in Solutions of Tetracoordinate Chelate Complexes of Nontransition Metals. *Russ. Chem. Rev.* **1994**, *63*, 289−311.

(30) Minkin, V. I.; Minyaev, R. M. Theoretical Study of Mechanisms of Polytopical Rearrangements of Molecules in Sulfurans and their Analogs. *Zh. Org. Khim.* **1975**, *11*, 1993−2001.

(31) Mauksch, M.; Schleyer, P. v. R. Effective Monkey Saddle Points and Berry and Lever Mechanisms in the Topomerization of SF_4 and Related Tetracoordinated AX_4 Species. *Inorg. Chem.* **2001**, *40*, 1756−1769.

(32) Zou, W.; Tao, Y.; Kraka, E. Describing Polytopal Rearrangements of Fluxional Molecules with Curvilinear Coordinates Derived from Normal Vibrational Modes: A Conceptual Extension of Cremer−Pople Puckering Coordinates. *J. Chem. Theory Comput.* **2020**, *16*, 3162−3193.

(33) Wakatsuki, Y.; Yamazaki, H. Formation of Dicyanocobaltacyclopentanes from a Cobalt(acrylonitrile) Complex and Isomerization of the *cis*-Isomers via a Polytopal Rearrangement. *J. Chem. Soc., Chem. Commun.* **1980**, 1270−1271.

(34) Farrugia, L. J. Novel Metal Framework Rearrangements in Mercury-bridged Cluster Complexes: X-ray crystal Structures of $[Hg\{Fe_2M(\mu_3\text{-}COMe)(CO)_7(\eta\text{-}C_5H_5)\}_2]$(M =Co and Rh). *J. Chem. Soc., Chem. Commun.* **1987**, 147−149.

(35) Tatsumi, K.; Nakamura, A.; Komiya, S.; Yamamoto, A.; Yamamoto, T. An Associative Mechanism for Reductive Elimination of d^8 $NiR_2(PR_3)_2$. *J. Am. Chem. Soc.* **1984**, *106*, 8181−8188.

https://doi.org/10.1021/acsorginorgau.4c00005
ACS Org. Inorg. Au 2024, 4, 356−372

(36) Minkin, V. I.; Pichko, V. A.; Abubikerova, I. A.; Simkin, B. Y. An MNDO Study of Mechanisms of Rapid Intramolecular Enantiomerization of *bis*-Chelate Hg(II) Complexes. *J. Mol. Struct.: THEOCHEM* **1991**, *227*, 295−304.
(37) Rzepa, H. S.; Cass, M. E. A Computational Study of the Nondissociative Mechanisms that Interchange Apical and Equatorial Atoms in Square Pyramidal Molecules. *Inorg. Chem.* **2006**, *45*, 3958−3963.
(38) Osborn, J. A.; Shapley, J. R. Rapid Intramolecular Rearrangements in Pentacoordinate Transition Metal Compounds. Rearrangement Mechanism of Some Fluxional Iridium(I) complexes. *J. Am. Chem. Soc.* **1970**, *92*, 6976−6978.
(39) Thorn, D. L.; Hoffmann, R. The Olefin Insertion Reaction. *J. Am. Chem. Soc.* **1978**, *100*, 2079−2090.
(40) Tatsumi, K.; Hoffmann, R.; Yamamoto, A.; Stille, J. K. Reductive Elimination of d^8-Organotransition Metal Complexes. *Bull. Chem. Soc. Jpn.* **1981**, *54*, 1857−1867.
(41) Cesar, V.; Bellemin-Laponnaz, S.; Gade, L. H. Cationic and Neutral Rhodium(I) Oxazolinylcarbene Complexes. *Eur. J. Inorg. Chem.* **2004**, *2004*, 3436−3444.
(42) Daul, C.; Niketic, S.; Rauzy, C.; Schläpfer, C.-W. Polytopal Rearrangement of $[Ni(acac)_2(py)]$: A New Square Pyramid⇆Trigonal Bipyramid Twist Mechanism. *Chemistry − A European Journal* **2004**, *10*, 721−727.
(43) Khan, R. K. M.; Zhugralin, A. R.; Torker, S.; O'Brien, R. V.; Lombardi, P. J.; Hoveyda, A. H. Synthesis, Isolation, Characterization, and Reactivity of High-Energy Stereogenic-at-Ru Carbenes: Stereochemical Inversion through Olefin Metathesis and Other Pathways. *J. Am. Chem. Soc.* **2012**, *134*, 12438−12441.
(44) Torker, S.; Khan, R. K. M.; Hoveyda, A. H. The Influence of Anionic Ligands on Stereoisomerism of Ru Carbenes and Their Importance to Efficiency and Selectivity of Catalytic Olefin Metathesis Reactions. *J. Am. Chem. Soc.* **2014**, *136*, 3439−3455.
(45) Asatryan, R.; Ruckenstein, E.; Hachmann, J. Revisiting the Polytopal Rearrangements in Pentacoordinate d^7-Metallocomplexes: Modified Berry Pseudorotation, Octahedral Switch, and Butterfly Isomerization. *Chemical Science* **2017**, *8*, 5512−5525.
(46) Minyaev, R. M.; Minkin, V. I. Theoretical Study of the Mechanism of Associative Nucleophilic Substitution in Compounds of Five-Coordinated Nontransition Elements of Groups V and VI. *Journal of Structural Chemistry* **1980**, *20*, 715−725.
(47) De Keijzer, A. E. H.; Koole, L. H.; Buck, H. M. Pseudorotation in Pentacoordinated Phosphorus Compounds. The Influence of the Conformational Transmission Effect on the Barriers to Pseudorotation in Cyclic Alkoxyphosphoranes. *J. Am. Chem. Soc.* **1988**, *110*, 5995−6001.
(48) Couzijn, E. P. A.; Slootweg, J. C.; Ehlers, A. W.; Lammertsma, K. Stereomutation of Pentavalent Compounds: Validating the Berry Pseudorotation, Redressing Ugi's Turnstile Rotation, and Revealing the Two- and Three-Arm Turnstiles. *J. Am. Chem. Soc.* **2010**, *132*, 18127−18140.
(49) Vancea, L.; Bennett, M. J.; Jones, C. E.; Smith, R. A.; Graham, W. A. G. Stereochemically Nonrigid Six-coordinate Metal Carbonyl Complexes. 1. Polytopal Rearrangement and X-ray Structure of Tetracarbonylbis(trimethylsilyl)iron. *Inorg. Chem.* **1977**, *16*, 897−902.
(50) Kreiter, C. G.; Özkar, S. Gehinderte Ligandenbewegungen in übergangsmetall-komplexen: XIV. Das dynamische vërhalten von η-dienchrom(0) - und molybdän(0)-komplexen. *J. Organomet. Chem.* **1978**, *152*, C13−C18.
(51) Kampe, C. E.; Boag, N. M.; Knobler, C. B.; Kaesz, H. D. Synthesis and Characterization of Edge-Double-Bridged $Ru_3(\mu\text{-H},\mu\text{-X})(CO)_{10}$ (X = Cl, Br, I) and Face-Triple-Bridged $Ru_3(\mu\text{-H},\mu_3\text{-I})(CO)_9$. Crystal and Molecular Structure of $Ru_3(\mu\text{-H},\mu\text{-Br})(CO)_{10}$, $Ru_3(\mu\text{-I})_2(CO)_{10}$ and $Ru_3(\mu\text{-H},\mu_3\text{-I})(CO)_9$. *Inorg. Chem.* **1984**, *23*, 1390−1397.
(52) Lee, C. Y.; Wang, Y.; Liu, C. S. Stereochemical Nonrigidity in Six-coordinate Monochelate Complexes via Polytopal Rearrangement. *Inorg. Chem.* **1991**, *30*, 3893−3899.
(53) Soubra, C.; Oishi, Y.; Albright, T. A.; Fujimoto, H. Intramolecular Rearrangements in Six-Coordinate Ruthenium and Iron Dihydrides. *Inorg. Chem.* **2001**, *40*, 620−627.
(54) Rzepa, H. S.; Cass, M. E. In Search of the Bailar and Rây−Dutt Twist Mechanisms That Racemize Chiral Trischelates: A Computational Study of Sc^{III}, Ti^{IV}, Co^{III}, Zn^{II}, Ga^{III}, and Ge^{IV} Complexes of a Ligand Analogue of Acetylacetonate. *Inorg. Chem.* **2007**, *46*, 8024−8031.
(55) Trindle, C.; Datta, S. N.; Bouman, T. D. Nonrigid Molecule Effects on the Energy Levels of XeF_6. *Int. J. Quantum Chem.* **1977**, *11*, 627−664.
(56) Hawthorne, S. L.; Fay, R. C. Stereochemically Rigid Seven-coordinate Complexes. Synthesis, Structure, and Dynamic Stereochemistry of Chlorotris(*N*,*N*-dialkylmonothiocarbamato)titanium(IV) complexes. *J. Am. Chem. Soc.* **1979**, *101*, 5268−5277.
(57) Dedieu, A. Theoretical Study of the Olefin Insertion Step in the Chlorotris(triphenylphosphine)rhodium(I)-catalyzed Hydrogenation of Olefins. *Inorg. Chem.* **1981**, *20*, 2803−2813.
(58) Fay, R. C.; Weir, J. R.; Bruder, A. H. Nuclear Magnetic Resonance Studies of Stereochemical Rearrangements in Pentagonal-Bipyramidal (η^5-Cyclopentadienyl)*tris*(*N*,*N*-dimethyl-dithiocarbamato)titanium-(IV), -Zirconium(IV), and -Hafnium(IV). *Inorg. Chem.* **1984**, *23*, 1079−1089.
(59) Burdett, J. K.; Hoffmann, R.; Fay, R. C. Eight-Coordination. *Inorg. Chem.* **1978**, *17*, 2553−2568.
(60) Fay, R. C.; Howie, J. K. Stereochemistry and Stereochemical Rearrangements of Eight-coordinate *tetrakis* Chelates. 1. Group 4B. β-Diketonates. *J. Am. Chem. Soc.* **1979**, *101*, 1115−1122.
(61) Weir, J. R.; Fay, R. C. Stereochemistry and Metal-centered Rearrangements of Eight-Coordinate Niobium(V) and Tantalum(V) Dithiocarbamates and Monothiocarbamates. *Inorg. Chem.* **1986**, *25*, 2969−2976.
(62) Gutowsky, H. S.; McCall, D. W.; Slichter, C. P. Nuclear Magnetic Resonance Multiplets in Liquids. *J. Chem. Phys.* **1953**, *21*, 279−292.
(63) Cotton, F. A.; Danti, A.; Waugh, J. S.; Fessenden, R. W. Carbon-13 Nuclear Resonance Spectrum and Low-Frequency Infrared Spectrum of Iron Pentacarbonyl. *J. Chem. Phys.* **1958**, *29*, 1427−1428.
(64) Jin, H.; Xie, J.; Pan, C.; Zhu, Z.; Cheng, Y.; Zhu, C. Rhenium-Catalyzed Acceptorless Dehydrogenative Coupling via Dual Activation of Alcohols and Carbonyl Compounds. *ACS Catal.* **2013**, *3*, 2195−2198.
(65) Jin, H.; Zhu, Z.; Jin, N.; Xie, J.; Cheng, Y.; Zhu, C. CO-Enabled Rhenium Hydride Catalyst for Directed $C(sp^2)$−H Bond Alkylation with Olefins. *Organic Chemistry Frontiers* **2015**, *2*, 378−382.
(66) Mislow, K. Role of Pseudorotation in the Stereochemistry of Nucleophilic Displacement Reactions. *Acc. Chem. Res.* **1970**, *3*, 321−331.
(67) Gorenstein, D.; Westheimer, F. H. Nuclear Magnetic Resonance Evidence for the Pathways of Pseudorotation in Alkyloxyphosphoranes. *J. Am. Chem. Soc.* **1970**, *92*, 634−644.
(68) Ballweg, D.; Liu, Y.; Guzei, I. A.; West, R. Pentacoordinate Spirosilicate Anion, *bis*(2,2′-Biphenyldiyl)methylsilicate, Synthesized by the Lithium Cleavage of Dimethoxyethane. *Silicon Chem.* **2002**, *1*, 55−58.
(69) Couzijn, E. P. A.; Ehlers, A. W.; Schakel, M.; Lammertsma, K. Electronic Structure and Stability of Pentaorganosilicates. *J. Am. Chem. Soc.* **2006**, *128*, 13634−13639.
(70) Matsukawa, S.; Yamamichi, H.; Yamamoto, Y.; Ando, K. Pentacoordinate Organoantimony Compounds That Isomerize by Turnstile Rotation. *J. Am. Chem. Soc.* **2009**, *131*, 3418−3419.
(71) Gromski, P. S.; Henson, A. B.; Granda, J. M.; Cronin, L. How to Explore Chemical Space Using Algorithms and Automation. *Nat. Rev. Chem.* **2019**, *3*, 119−128.
(72) Lipinski, C.; Hopkins, A. Navigating Chemical Space for Biology and Medicine. *Nature* **2004**, *432*, 855−861.
(73) Dobson, C. M. Chemical Space and Biology. *Nature* **2004**, *432*, 824−828.
(74) Baldi, P. Call for a Public Open Database of All Chemical Reactions. *J. Chem. Inf. Model.* **2022**, *62*, 2011−2014.

https://doi.org/10.1021/acsorginorgau.4c00005
ACS Org. Inorg. Au 2024, 4, 356−372

(75) Ray, P.; Dutt, N. Kinetics and Mechanism of Racemization of Optically Active Cobaltic *trisBiguanide* Complex. *J. Indian Chem. Soc.* **1943**, *20*, 81−92.
(76) Bailar, J. C. Some Problems in the Stereochemistry of Coordination Compounds: Introductory Lecture. *Journal of Inorganic and Nuclear Chemistry* **1958**, *8*, 165−175.
(77) Muetterties, E. L.; Phillips, W. D. Structure of ClF_3 and Exchange Studies on Some Halogen Fluorides by Nuclear Magnetic Resonance1. *J. Am. Chem. Soc.* **1957**, *79*, 322−326.
(78) Muetterties, E. L.; Phillips, W. D. Structure and Exchange Processes in Some Inorganic Fluorides by Nuclear Magnetic Resonance1. *J. Am. Chem. Soc.* **1959**, *81*, 1084−1088.
(79) Miller, H. C.; Miller, N. E.; Muetterties, E. L. Synthesis of Polyhedral Boranes. *J. Am. Chem. Soc.* **1963**, *85*, 3885−3886.
(80) Muetterties, E. L.; Packer, K. J. Intramolecular Ligand Exchange in Seven-Coordinate Structures. *J. Am. Chem. Soc.* **1964**, *86*, 293−294.
(81) Miller, H. C.; Muetterties, E. L.; Boone, J. L.; Garrett, P.; Hawthorne, M. F. Borane Anions. *In Inorg. Synth.* **1967**, *10*, 81−91.
(82) Hawthorne, M. F. Boron Compounds. *Science* **1968**, *161*, 153−153.
(83) Gordon, J. P.; Zeiger, H. J.; Townes, C. H. The Maser—New Type of Microwave Amplifier, Frequency Standard, and Spectrometer. *Phys. Rev.* **1955**, *99*, 1264−1274.
(84) Berry, R. S. Correlation of Rates of Intramolecular Tunneling Processes, with Application to Some Group V Compounds. *J. Chem. Phys.* **1960**, *32*, 933−938.
(85) Hoard, J. L.; Silverton, J. V. Stereochemistry of Discrete Eight-Coördination. I. Basic Analysis. *Inorg. Chem.* **1963**, *2*, 235−242.
(86) Lipscomb, W. N. Framework Rearrangement in Boranes and Carboranes. *Science* **1966**, *153*, 373−378.
(87) Holmes, R. R.; Deiters, S. R. M. Intramolecular Exchange in Phosphorus Pentahalide Molecules. *J. Am. Chem. Soc.* **1968**, *90*, 5021−5023.
(88) Udovich, C. A.; Clark, R. J. Stereochemical Nonrigidity in Phosphorus Trifluoride Substituents of Trifluoromethylcobalt Tetracarbonyl. *J. Am. Chem. Soc.* **1969**, *91*, 526−527.
(89) Cahoon, J. F.; Sawyer, K. R.; Schlegel, J. P.; Harris, C. B. Determining Transition-State Geometries in Liquids Using 2D-IR. *Science* **2008**, *319*, 1820−1823.
(90) Campbell, B. S.; De'Ath, N. J.; Denney, D. B.; Denney, D. Z.; Kipnis, I. S.; Min, T. B. Some Caged Polycyclic Phosphoranes. *J. Am. Chem. Soc.* **1976**, *98*, 2924−2927.
(91) Couzijn, E. P. A.; Schakel, M.; de Kanter, F. J. J.; Ehlers, A. W.; Lutz, M.; Spek, A. L.; Lammertsma, K. Dynamic Configurational Isomerism of a Stable Pentaorganosilicate. *Angew. Chem., Int. Ed.* **2004**, *43*, 3440−3442.
(92) de Keijzer, A. H. J. F.; de Kanter, F. J. J.; Schakel, M.; Osinga, V. P.; Klumpp, G. W. In Search of Stable Lithium Pentaorganylsilicates; Special Role of Five Phenyl Ligands and of Ligands Containing the 1,4-(1,3-Butadienediyl) Unit. *J. Organomet. Chem.* **1997**, *548*, 29−32.
(93) Couzijn, E. P. A.; van den Engel, D. W. F.; Slootweg, J. C.; de Kanter, F. J. J.; Ehlers, A. W.; Schakel, M.; Lammertsma, K. Configurationally Rigid Pentaorganosilicates. *J. Am. Chem. Soc.* **2009**, *131*, 3741−3751.
(94) Udovich, C. A.; Krevalis, M. A.; Clark, R. J. Metal Carbonyl-phosphorus Trifluoride Systems. XIII. Fluorine Nuclear Magnetic Resonance Studies on $R_fCo(PF_3)_x(CO)_{4-x}$ Compounds (R_f = Trifluoromethyl, Pentafluoroethyl, Heptafluoropropyl). *Inorg. Chem.* **1976**, *15*, 900−905.
(95) Eyring, H.; Walter, J.; Kimball, G. E. *Quantum chemistry*; Wiley: New York, 1944.
(96) Hoskins, L. C.; Lord, R. C. Vibrational Spectra of PF_5 and AsF_5: Height of the Barrier to Internal Exchange of Fluorine Nuclei. *J. Chem. Phys.* **1967**, *46*, 2402−2412.
(97) Tao, Y.; Zou, W.; Luo, G.-G.; Kraka, E. Describing Polytopal Rearrangement Processes of Octacoordinate Structures. I. Renewed Insights into Fluxionality of the Rhenium Polyhydride Complex $ReH_5(PPh_3)_2$(Pyridine). *Inorg. Chem.* **2021**, *60*, 2492−2502.
(98) Moberg, C. Stereomutation in Trigonal-Bipyramidal Systems: A Unified Picture. *Angew. Chem., Int. Ed.* **2011**, *50*, 10290−10292.
(99) Martin, L. D.; Perozzi, E. F.; Martin, J. C. Sulfuranes. 39. Syntheses and Structure Studies of Stable Difluoro- and Dichlorosulfuranes. Apicophilicity Orders in Sulfuranes. *J. Am. Chem. Soc.* **1979**, *101*, 3595−3602.
(100) Martin, J. C.; Balthazor, T. M. Sulfuranes. 22. Stereochemical Course of an Associative Displacement at Tetracoordinate Sulfur(IV) in a Sulfurane of Known Absolute Configuration. A Proposed System of Nomenclature for Optically Active Pentacoordinate Species. *J. Am. Chem. Soc.* **1977**, *99*, 152−162.
(101) Martin, J. C.; Perozzi, E. F. Sulfuranes. XII. Relative Reactivities of Acyclic, Cyclic and Spirobicyclic Sulfuranes and Sulfurane Oxides. *J. Am. Chem. Soc.* **1974**, *96*, 3155−3168.
(102) Astrologes, G. W.; Martin, J. C. Sulfuranes. XXI. Pseudorotation and Fragmentation of Perfluoropinacol Orthosulfite. A Tetraoxysulfurane. *J. Am. Chem. Soc.* **1976**, *98*, 2895−2900.
(103) Fukui, K. The Path of Chemical-Reactions - The IRC Approach. *Acc. Chem. Res.* **1981**, *14*, 363−368.
(104) Alvarez, S.; Avnir, D.; Llunell, M.; Pinsky, M. Continuous Symmetry Maps and Shape Classification. The Case of Six-Coordinated Metal Compounds. *New J. Chem.* **2002**, *26*, 996−1009.
(105) Zabrodsky, H.; Peleg, S.; Avnir, D. Continuous Symmetry Measures. *J. Am. Chem. Soc.* **1992**, *114*, 7843−7851.
(106) Casanova, D.; Cirera, J.; Llunell, M.; Alemany, P.; Avnir, D.; Alvarez, S. Minimal Distortion Pathways in Polyhedral Rearrangements. *J. Am. Chem. Soc.* **2004**, *126*, 1755−1763.
(107) Cremer, D.; Pople, J. A. General Definition of Ring Puckering Coordinates. *J. Am. Chem. Soc.* **1975**, *97*, 1354−1358.
(108) Zou, W.; Izotov, D.; Cremer, D. New Way of Describing Static and Dynamic Deformations of the Jahn−Teller Type in Ring Molecules. *J. Phys. Chem. A* **2011**, *115*, 8731−8742.
(109) Brecher, J. Graphical Representation of Stereochemical Configuration (IUPAC Recommendations 2006). *Pure Appl. Chem.* **2006**, *78*, 1897−1970.
(110) Moss, G. P. Basic Terminology of Stereochemistry. *Pure Appl. Chem.* **1996**, *68*, 2193−2222.
(111) Connelly, N. G.; Damhus, T.; Hartshorn, R.; Hutton, A. T. *IUPAC Red Book*; RSC Publishing: London, 2005.
(112) Gielen, M., Applications of Graph Theory to Organometallic Chemistry. In *Chemical applications of graph theory*; Balaban, A. T., Ed;. Academic Press: London, 1976; pp 261−298.
(113) Balaban, A. T. *Chemical applications of graph theory*; Academic Press: London, 1976.
(114) Amigó, J. M.; Gálvez, J.; Villar, V. M. A Review on Molecular Topology: Applying Graph Theory to Drug Discovery and Design. *Naturwissenschaften* **2009**, *96*, 749−761.
(115) Sporns, O. Graph Theory Methods: Applications in Brain Networks. *Dialogues in Clinical Neuroscience* **2018**, *20*, 111−121.
(116) Phillips, J. D.; Schwanghart, W.; Heckmann, T. Graph Theory in the Geosciences. *Earth-Science Reviews* **2015**, *143*, 147−160.
(117) Zhang, W.; Chien, J.; Yong, J.; Kuang, R. Network-based Machine Learning and Graph Theory Algorithms for Precision Oncology. *npj Precision Oncology* **2017**, *25*, 1−15.
(118) Chulahwat, A. Capturing Building Vulnerability to Wildfires with Graph Theory. *Nat. Rev. Earth Environ.* **2023**, *4*, 600.
(119) Bradlyn, B.; Elcoro, L.; Vergniory, M. G.; Cano, J.; Wang, Z.; Felser, C.; Aroyo, M. I.; Bernevig, B. A. Band Connectivity for Topological Quantum Chemistry: Band Structures as a Graph Theory Problem. *Phys. Rev. B* **2018**, *97*, No. 035138.
(120) Derrible, S.; Kennedy, C. Applications of Graph Theory and Network Science to Transit Network Design. *Transport Reviews* **2011**, *31*, 495−519.
(121) *CAS DATA*. https://www.cas.org/cas-data (accessed 2 August 2023).

https://doi.org/10.1021/acsorginorgau.4c00005
ACS Org. Inorg. Au 2024, 4, 356−372